HHS Public Access

Author manuscript

J Comp Neurol. Author manuscript; available in PMC 2018 July 01.

Published in final edited form as:

J Comp Neurol. 2017 July 01; 525(10): 2287–2309. doi:10.1002/cne.24215.

Barrington's nucleus: Neuroanatomic landscape of the mouse "pontine micturition center"

Anne M. J. Verstegen[1,2,3], **Veronique Vanderhorst**[3,4], **Paul A. Gray**[5,6], **Mark L. Zeidel**[1,3], and **Joel C. Geerling**[3,4]

[1]Department of Medicine, Beth Israel Deaconess Medical Center, Boston, Massachusetts

[2]Division of Endocrinology, Beth Israel Deaconess Medical Center, Boston, Massachusetts

[3]Department of Medicine & Neurology, Harvard Medical School, Boston, Massachusetts

[4]Department of Neurology, Beth Israel Deaconess Medical Center, Boston, Massachusetts

[5]Department of Anatomy & Neurobiology, Washington University School of Medicine, Saint Louis, Missouri

[6]Indigo Ag, Inc., Charlestown, Massachusetts

Abstract

Barrington's nucleus (Bar) is thought to contain neurons that trigger voiding and thereby function as the "pontine micturition center." Lacking detailed information on this region in mice, we examined gene and protein markers to characterize Bar and the neurons surrounding it. Like rats and cats, mice have an ovoid core of medium-sized Bar neurons located medial to the locus coeruleus (LC). Bar neurons express a GFP reporter for *Vglut2*, develop from a *Math1/Atoh1* lineage, and exhibit immunoreactivity for NeuN. Many neurons in and around this core cluster express a reporter for corticotrophin-releasing hormone (Bar^{CRH}). Axons from Bar^{CRH} neurons project to the lumbosacral spinal cord and ramify extensively in two regions: the dorsal gray commissural and intermediolateral nuclei. Bar^{CRH} neurons have unexpectedly long dendrites, which may receive synaptic input from the cerebral cortex and other brain regions beyond the core afferents identified previously. Finally, at least five populations of neurons surround Bar: rostral-dorsomedial cholinergic neurons in the laterodorsal tegmental nucleus; lateral noradrenergic neurons in the LC; medial GABAergic neurons in the pontine central gray; ventromedial, small GABAergic neurons that express FoxP2; and dorsolateral glutamatergic neurons that express FoxP2 in the pLC and form a wedge dividing Bar from the dorsal LC. We discuss the implications of this new information for interpreting existing data and future experiments targeting Bar^{CRH} neurons and their synaptic afferents to study micturition and other pelvic functions.

Correspondence: Joel C. Geerling, 200 Hawkins Dr. – 1320 PBDB, Iowa City, IA 52242-1009. joel-geerling@uiowa.edu.

CONFLICT OF INTEREST

The authors declare that they have no conflicts of interest.

AUTHOR CONTRIBUTIONS

All authors had full access to all the data in the study and take responsibility for the integrity of the data and the accuracy of analysis. Study concept and design: AV, VV, MZ, JCG. Acquisition of data: AV, PAG, JCG. Analysis and interpretation of data: AV, VV, JCG. Drafting of the manuscript: JCG. Critical revision of the manuscript for important intellectual content: AV, VV, MZ, JCG. Statistical analysis: n/a. Obtained funding: MZ. Administrative, technical, and material support: AV, VV, MZ, JCG. Study supervision: MZ, JCG.

Keywords

bladder; continence; dorsal gray commissure nucleus; FoxP2; locus coeruleus; pontospinal; math1/atoh1; micturition; neuroanatomy; neurourology; pelvic autonomic; pontine central gray; pre-locus coeruleus; sacral intermediolateral nucleus; urethral sphincter; voiding

1 INTRODUCTION

A small region of the upper brainstem, within the lateral pontine tegmentum, is critical for normal voiding behavior in cats (Barrington, 1921, 1925, 1927), rats (Satoh, Shimizu, Tohyama, & Maeda, 1978), and humans (Fowler, 1999; Sakakibara, 2015; Ueki, 1960). This region is located between the locus coeruleus (LC) and laterodorsal tegmental nucleus (LDT) and contains a small number of neurons that increase their activity in response to bladder distention (Rouzade-Dominguez, Pernar, Beck, & Valentino, 2003). Immediately before the bladder contracts, these neurons begin firing, and they sustain this activity throughout the contraction and in close correspondence to bladder pressure (Hou et al., 2016; Tanaka et al., 2003). Injecting electric current or glutamate in this region triggers micturition (Kruse, Mallory, Noto, Roppolo, & de Groat, 1991; Mallory, Roppolo, & de Groat, 1991; Mallory & Steers, 1989; Nishizawa, Sugaya, Noto, Harada, & Tsuchida, 1988; Sugaya, Matsuyama, Takakusaki, & Mori, 1987), while inhibition of or injury to this region prevents voiding, causing urinary retention in rats, cats, and humans (Barrington, 1925; Komiyama, Kubota, & Hidai, 1998; Mallory et al., 1991; Satoh, Shimizu, et al., 1978).

These findings gave rise to the concept in rats that the pontine tegmentum contains a "pontine micturition center," or PMC (Loewy, Saper, & Baker, 1979; Sugaya et al., 1987), which in cats was called the "pontine detrusor nucleus" (Kuru & Yamamoto, 1964) or "M-region" (Holstege, Griffiths, de Wall, & Dalm, 1986). Each term conveys the notion that a population of neurons integrates a stretch signal from the bladder with other contextual information and, via long axonal projections to the spinal cord, coordinates bladder contraction with relaxation of the urethral sphincter (Kruse et al., 1991; Mallory et al., 1991).

Very few tegmental neurons have bladder-related activity, and they are surrounded by and intermingle with much larger populations of unrelated neurons (Tanaka et al., 2003; Yamao, Koyama, Akihiro, Yukihiko, & Tsuneharu, 2001). Due to a paucity of markers for these diverse neuron populations, conflicting opinions arose about which features distinguish the PMC. More than one population of neurons was said to function as the PMC based on sites where electrical stimulation, lesions, or drug injection alter voiding. However, the anatomic resolution of these techniques cannot distinguish among the myriad, intermingled populations of neurons in this region of the brainstem, which form sub-millimeter, overlapping distributions. Nonetheless, with limited histochemical markers, some investigators proposed that the PMC consists of catecholaminergic neurons in the LC or subcoeruleus (Kuru & Yamamoto, 1964; Mallory et al., 1991; Nishizawa et al., 1988; Sugaya et al., 1987), or cholinergic neurons in the LDT (Noto, Roppolo, Steers, & de Groat, 1991; Satoh, Shimizu, et al., 1978).

Axonal tracing in rats identified a third, unmarked, cluster of neurons centered between the LC and LDT. Like catecholamine neurons in the ventral LC and subcoeruleus, these neurons send long axonal projections to lumbosacral levels of the spinal cord, yet they survived chemical toxins that destroy catecholamine neurons (Loewy et al., 1979; Satoh, Tohyama, Sakumoto, Yamamoto, & Shimizu, 1978; Tohyama et al., 1978). Further, lesions in the LC had no effect on micturition, while lesions targeting this newly identified cluster caused urinary retention in rats (Satoh, Shimizu, et al., 1978). Thus, many investigators concluded that PMC function, at least in rats, relied on noncatecholamine neurons located just rostral and medial to the LC.

In honor of F.J.F. Barrington, who first localized micturition to the pontine tegmentum using focal lesions in cats (Barrington, 1921, 1925, 1927), we and most neuroanatomists refer to this population of spinally projecting, noncatecholamine neurons as *Barrington's nucleus*, typically abbreviated "*Bar*" (Dong & The Allen Institute for Brain Science, 2008; Paxinos & Franklin, 2008; Standaert, Needleman, & Saper, 1986), while others still refer to it or the region around it as the PMC. Bar neurons probably are critical for triggering micturition, but they may also influence other pelvic functions, given their extensive projections to the sacral IML and the observation that some are activated equally by distention of the bladder or colon (Rouzade-Dominguez et al., 2003).

Bar includes a subpopulation of neurons that express corticotropin releasing hormone (Imaki, Nahan, Rivier, Sawchenko, & Vale, 1991; Valentino et al., 1994; Vincent & Satoh, 1984). In rats, almost half of all Bar neurons are immunoreactive for this neuropeptide, including more than 40% of those that project to the spinal cord (Valentino, Pavcovich, & Hirata, 1995), so CRH became a de facto marker for this population (Rizvi et al., 1994; Rouzade-Dominguez et al., 2003; Valentino et al., 1994).

Now, mice are the species of choice for conditionally targeting specific cell populations, but our ability to harness genetically targeted techniques to study micturition is hampered by a lack of detailed information about the location and identity of Bar neurons in this species. Recombinase-based targeting allows us to express receptors, opsins, tracers, and other experimental tools in genetically defined populations of neurons, but designing and interpreting experiments using these techniques requires a solid foundation of neuroanatomical information. Before targeting Bar neurons as an entry point to studying the larger-scale circuits controlling micturition, it is important that we understand the location and distribution of any markers shared by or distinguishing Bar and surrounding neurons. This information is particularly important because Bar sits in one of the most complex regions of the brainstem, where our knowledge of genetic markers remains fragmentary.

To help fill the gaps, we used Cre-reporter mice, Cre-conditional expression of fluorescent proteins, and immunofluorescence labeling to identify markers for Bar and surrounding neurons in the mesopontine tegmentum. The primary goal of this study was to provide detailed information on the location, gene expression, and spinal projections of Bar^{CRH} neurons, using *Crh-IRES-Cre* mice. This information is essential for planning and interpreting experiments accessing Bar neurons as a gateway to the brain circuitry controlling micturition.

2 MATERIALS AND METHODS

2.1 Mice

Mice used in this study were bred on a mixed background composed of primarily C57/B6J (The Jackson Laboratory). Specifically for this study, we prepared and imaged tissue from *n* = 27 adult mice to provide neuroanatomic information for on-going micturition physiology work. Except where otherwise specified, mice weighed between 20 and 29 g. Exact numbers for each genotype used for specific experiments are detailed below.

To label Bar neurons expressing CRH (Bar^{CRH}), we used adult male and female *Crh-IRES-Cre; R26-lsl-L10-GFP* mice (*n* = 3, 22–28 g). In these mice, cells expressing the gene *Crh* produce Cre-recombinase. Cre-recombinase expression at any developmental age will induce L10-GFP expression from the *Rosa26* (*R26*) locus by permanently excising the *loxSTOPlox* (*lsl*) sequence. L10-GFP is a fusion protein between GFP and the ribosomal L10 subunit (Krashes et al., 2014), which restricts GFP labeling into the cell soma and proximal dendrites. The L10-GFP reporter produces excellent cell body labeling, with no axonal labeling, in contrast to the variable distributions of other fluorescent reporters in cells and axons. In this "CRH reporter" strain, the distribution of L10-GFP throughout the brain was shown in supplementary figure 7b in Krashes et al. (Krashes et al., 2014). The distribution of this CRH reporter is similar to that of *Crh* mRNA and CRH immunoreactivity (Krashes et al., 2014; Lein et al., 2007; Swanson, Sawchenko, Rivier, & Vale, 1983). *Crh-IRES-Cre* and *R26-lsl-L10-GFP* knock-in mice were generated by Dave Olsen (Krashes et al., 2014) and used with permission from the Lowell laboratory at BIDMC.

To label the dendrites of Bar^{CRH} neurons, we injected adult, male *Crh-IRES-Cre* mice (23–26 g, *n* = 6; no GFP reporter, see "Stereotaxic injections" below). To label axonal projections from Bar^{CRH} neurons to the spinal cord, and to label autonomic preganglionic and somatomotor neurons in the spinal cord, we used female *Crh-IRES-Cre; Chat-GFP* mice (*n* = 2). In addition to expressing Cre in Bar^{CRH} neurons, these mice contain a BAC transgene with GFP after the promotor for choline acetyltransferase (Tallini et al., 2006).

To label glutamatergic and GABAergic neurons, we also examined L10-GFP reporter mice for the glutamatergic marker *Vglut2* (type 2 vesicular glutamate transporter; *n* = 2, *Vglut2-IRES-Cre; R26-lsl-L10-GFP*) and for the GABA/glycine marker *Vgat* (vesicular GABA/glycine transporter; n = 2, *Vgat-IRES-Cre; R26-lsl-L10-GFP*). *Vglut2-IRES-Cre* and *Vgat-IRES-Cre* mice were generated by Linh Vong (Vong et al., 2011) and used with permission from the Lowell laboratory.

Finally, to fate-map neuronal lineages derived from *Math1*/*Atoh1*-expressing embryonic precursors, we crossed *Atoh1-Cre* mice (Chen, Johnson, Zoghbi, & Segil, 2002) with a *Rosa26-stop-EYFP* Cre-reporter (Srinivas et al., 2001) bred on a mixed CD1/C56B6 background. We examined tissue from n = 10 progeny, including *n* = 4 in detail, as described below. These experiments were done in accordance with the Institute for Laboratory Animal Research Guide for the Care and Use of Laboratory Animals and approved by the Animal Studies Committee at Washington University School of Medicine.

2.2 Mouse husbandry

Mice were housed in our barrier facility at BIDMC, with the exception of *Atoh1* reporter mice, which were housed at Washington University School of Medicine. Littermates were weaned at 21 days and group-housed with up to five mice in each cage. Cages were kept in ventilated racks in air-sealed rooms with stable air temperature (21–23°C), humidity (30–40%), and a 12/12-hr light-dark cycle. Each cage contained corncob bedding and nesting material. Water and standard rodent chow were available ad libitum. The BIDMC IACUC approved all husbandry and experimental protocols.

2.3 Stereotaxic injections

Under ketamine-xylazine anesthesia (100 mg/kg and 10 mg/kg), we made stereotaxic injections targeting Bar. Bilateral AAV injections were made using the following coordinates: 5.40 caudal to bregma, lateral 0.68 mm, and 3.70 deep to bregma. Using controlled puffs of compressed air through a pulled glass micropipette (tip ~20 μm internal diameter), we injected 25–50 nl of AAV9-CBA-DIO-ChR2(H134R)-mCherry ($n = 2$ mice; K. Diesseroth, U Penn Vector Core) or 25–50 nl AAV8-hSyn-DIO-hM3Dq-mCherry ($n = 3$ mice; B. Roth, UNC Vector Core). Postoperatively, we administered meloxicam (5 mg/kg s.c.) and observed the mice on a heating pad until they recovered spontaneous locomotion. After 4–6 weeks to allow protein production and transport into dendrites and axons, mice were perfused as described below.

In CRH reporter mice (*Crh-IRES-Cre; R26-lsl-L10-GFP*, 8–12 wks old), after a low lumbar ($n = 2$) or thoracic ($n = 2$) laminectomy as described before (VanderHorst, Gustafsson, & Ulfhake, 2005; Vander-Horst & Ulfhake, 2006), we made air pressure microinjections of cholera toxin b subunit (CTb) into the sacral or thoracic spinal cord. Using a fine-tipped glass micropipette, we injected approximately 100 nl of CTb (0.1% in ddH2O, Life Technologies). Mice were perfused after allowing 5 days for retrograde transport to the brainstem.

2.4 Perfusion and tissue sections

We anesthetized adult mice with chloral hydrate (7% in sterile saline, ~200 μl i.p., dosed by weight: 0.8 * BW in g * 10 μl) then perfused phosphate-buffered saline (PBS) through the heart at room temperature, followed by 10% formalin-PBS (Fisher Scientific; Waltham, MA). We removed each brain immediately and fixed it overnight in 10% formalin-PBS at 4°C. After cryoprotection in 20% sucrose-PBS for 24 hr, we sectioned the brain or rostral brainstem, and in some cases the full spinal cord. Using a freezing microtome, we cut 30 or 40 μm-thick tissue sections in a 1-in-4 or 1-in-3 series, respectively. Sections were stored in cryoprotectant solution at −20°C or in PBS-azide at 4°C before immunofluorescence labeling, typically within 24–48 hr of slicing.

Neonatal pups (P0) were anesthetized by hypothermia and perfused transcardially with at least 10 ml paraformaldehyde-PBS, pH 7.4. Isolated brainstems were postfixed overnight at 4°C, then cryoprotected in 25% sucrose-PBS, blocked, frozen in embedding medium, and stored at −75°C. Brainstems were sectioned from the midbrain to the cervical spinal cord in

sets of six on a Hacker (Winnsboro, SC) cryostat at 20 μm and sections were thaw mounted onto Superfrost Plus slides and stored at −20°C until use.

2.5 Immunofluorescence histology

All antisera used in this study are listed in Table 1. Our protocols with anti-GFP, -mCherry, and -dsRed antisera did not produce any immunolabeling above background fluorescence in brain sections from mice that do not express GFP or that did not receive an AAV injection expressing mCherry. Likewise, the goat- and rabbit-anti-CTb antisera did not produce any labeling above background fluorescence in brain sections from mice without CTb injections, or in regions without established connectivity to the injection site in a given case. The sheep and goat FoxP2 antisera produced the same pattern of labeling we have analyzed and published in the mesopontine tegmentum of rats and mice (Geerling et al., 2011, 2016; Gray, 2008). Our goat anti-ChAT and our rabbit, sheep, and mouse anti-TH antisera all labeled well-established distributions of cholinergic or catecholaminergic neurons and axons, the one exception being that the mouse anti-TH antibody densely labeled pial tissue antigens along the periphery of all brain sections, but this did not interfere with identification of TH-immunoreactive neurons in the subcoeruleus and LC, near Bar.

We viewed and imaged L10-GFP using its native fluorescence (without immunolabeling), but we enhanced the relatively weak *ChAT-GFP* fluorescence in spinal cholinergic neurons by immunolabeling for GFP. We viewed mCherry initially by its native fluorescence to identify injection sites, but immunofluorescence labeling was necessary to see distal dendrites and axons above background fluorescence.

Our protocols for double- and triple-immunofluorescence labeling were similar to those described in greater detail in (Geerling et al., 2016). In brief, we rinsed sections twice in PBS, then placed them in netwells in a primary solution containing PBS with Triton 0.3% X-100 (PBT) along 2% normal horse serum (NHS) and one to three of the primary antisera listed in Table 1, which we selected to avoid any same-species cross-reactivity and to avoid goat/sheep cross-reactivity. We incubated sections overnight on a tissue shaker at room temperature. In the morning, we washed sections three times in PBS for 5 min each, then placed them in a secondary solution containing PBT with NHS plus one to three secondary antisera specific to the species of each primary antiserum. Secondary antisera were conjugated to Alexa555 (red/orange), Cy3 (red/orange), Alexa488 (green), or Alexa647 (far-red/infrared). We used AffiniPure donkey antisera from Jackson Immunore-search (West Grove, PA) at dilutions of 1:500 or 1:1,000, but in some cases we also used fluorophore-conjugated secondary antisera from Clontech or Invitrogen, again at dilutions 1:500 or 1:1,000. For some far-red labeling, we used a biotinylated secondary antiserum from Jackson, followed (after three PBS washes) by incubation for 1 hr in Cy5-streptavidin (Molecular Probes, #SA1011; diluted in PBT 1:1,000). No specific staining is seen in the absence of any primary antibody. After two final PBS washes, sections were mounted on glass slides, dried for at least an hour, and then coverslipped using Vectashield with DAPI (Vector Labs). We imaged slides immediately when possible, or stored them at 4°C in slide folders for up to several days before imaging.

For P0 tissue from *Atoh1* EYFP reporter mice ($n = 4$), we immuno-stained slides from one 1/6 series of brainstem sections using primary antibodies listed in Table 1 for GFP and FoxP2. Double-immunofluorescence labeling of slide-mounted p0 brain tissue included FITC-anti-chicken and Cy3-anti-goat secondaries from (Jackson) in a protocol similar to the above (Gray, 2013).

2.6 Nissl staining

We counterstained tissue from *Crh-IRES-Cre; R26-lsl-L10-GFP* mice using a standard protocol. After whole-slide fluorescence imaging (below), we used xylene to remove coverslips from two cases (including that shown in Figure 1) then placed the slides in deionized water (ddH2O) for 3 min. After immersing the slides in thionin solution for 30 s, we returned them to ddH2O and flushed the chamber with tap water. Slides were then immersed serially in 50, 70, and 95% ethanol (2 min each), followed by 95% ethanol with dilute acetic acid (10 drips in 400 ml) for 45 s. From there, slides were placed in 100% ethanol ×2 (2 min each), followed by xylenes (3–5 min ×2). We then re-coverslipped the slides with Cytoseal (Richard-Allan Scientific), and reimaged them using brightfield microscopy. After Nissl staining, GFP fluorescence was no longer visible.

2.7 Imaging and figures

Fluorescent images of P0 hindbrain sections were acquired using a Nikon 90i microscope (Nikon Instruments, Melville, NY), Roper H2 cooled CCD camera (Photometrics, Tucson, AZ), and Optigrid Structured Illumination Confocal with a Prior (Rockland, MA) motorized translation stage. Pseudo-colored images were acquired in Volocity (Perkin Elmer, Waltham, MA), and modified in Photoshop (Adobe, San Jose, CA) or ImageJ (National Institutes of Health, Bethesda, MD) and exported as 8 bit JPEG images. Images were filtered and levels were adjusted for clarity.

All other data were acquired using fluorescence or brightfield whole-slide imaging with a 10× objective on a slide-scanning microscope (VS120, Olympus). We exported grayscale images from each color channel in OlyVIA v2.6 (Olympus). Images were cropped, contrast-adjusted, and assigned a color channel in Adobe Photoshop CS3. In select cases with air bubbles, scratches, or other artifacts, if the artifact was located outside the tissue section it was either cropped or eliminated using the rubber stamp tool; artifacts overlying tissue were left intact. To produce the images in the right-hand column of Figure 1, GFP-DAPI fluorescence images taken prior to thionin were aligned to brightfield photomicrographs of the same sections after counterstaining, and then the images were blended together from separate Photoshop layers. We made all drawings, labeling, and figure layouts in Adobe Illustrator CS3.

3 RESULTS

3.1 Mouse Bar neurons

In mouse Nissl preparations, the pontine tegmentum is largely similar to rats, with one major difference: the locus coeruleus (LC) is proportionally larger in mice. Relative to surrounding structures, the mouse LC is both taller (dorsal-ventral) and longer (rostral-caudal). Given

that LC is a major landmark easily identified in Nissl preparations, this rat-mouse difference demands extra attention to any nomenclature derived from spatial relationships to the LC in rats. For example, unlike rats where most Bar neurons are rostral to the LC (Valentino et al., 1994), in mice Bar and LC are found at the same rostrocaudal levels except the far-caudal end of the LC (Figures 1 and 2).

Despite these differences, mice do contain an ovoid cluster of medium-sized neurons medial to the LC (Figure 1c), similar to the "core" of Bar in rats (Valentino et al., 1994). From a 1-in-3 series of 40 μm-thick sections, the core of Bar in mice spans just one or two rostrocaudal levels (100–200 μm), and rostral or caudal to these levels we cannot distinguish Bar from other neurons in the tegmentum or reticular formation based on just their cytoarchitectural appearance, as in rats (Valentino et al., 1994). Thus, identifying Bar neurons outside the core requires a marker.

Here we use a green-fluorescent Cre-reporter for CRH expression to reveal the distribution of Bar^{CRH} neurons, acknowledging that admixed, non-CRH-expressing neurons (or CRH neurons failing to express the Cre-reporter) may also function as part of the same population. In L10-GFP reporter mice (*Crh-IRES-Cre; R26-lsl-L10-Gfp*), the Bar^{CRH} population is centered in the core of Bar with an overall distribution homologous to immunoreactivity for CRH peptide or in situ hybridization for *Crh* mRNA in rats (Rizvi et al., 1994; Rouzade-Dominguez et al., 2003; Valentino et al., 1994; Vincent & Satoh, 1984). Outside the core, this population extends rostral, ventral, and slightly caudal. The overall distribution of Bar^{CRH} neurons is approximately 0.5 mm tall (dorsal-ventral) by 0.25 mm wide (medial-lateral) and 0.6 mm long (rostral-caudal). Every CRH reporter mouse we have examined (male and female, across many litters) contained GFP-expressing neurons in this same bilateral distribution.

Outside Bar, only the reticular tegmental nucleus contained a prominent cluster of GFP+ neurons at these levels of the hindbrain (Figure 1a2–c2). Fewer, small GFP-expressing neurons were also scattered near the caudal, ventrolateral tip of the parabrachial nucleus (PB), in the vestibular nuclei, in the pontine nuclei, and along the margins of the principal sensory trigeminal nucleus (not shown).

3.2 Proximity to locus coeruleus

Bar closely approximates the LC in Nissl preparations (Figure 1). At every rostrocaudal level of the Bar^{CRH} population, the medial-ventral LC cradles the lateral aspect of Bar (Figure 2) except where a small wedge of unlabeled tissue separates the dorsolateral core of Bar from the dorsal LC (dashed outline in Figure 2d). Rostrally, small numbers of Bar^{CRH} neurons extend all the way to the rostral pole of the LC (Figure 2b), but not as far as the large, sparse catecholamine neurons that extend rostrally from the LC into the ventrolateral periaqueductal gray matter (Figure 2a). Caudally, Bar^{CRH} neurons do not extend all the way to the caudal pole of the LC (Figure 2f). Nowhere in this region do any neurons express both GFP and TH so, despite close proximity and similar to rats, LC and Bar^{CRH} neurons in mice are entirely separate populations.

3.2.1 NeuN—TH-immunofluorescence is useful as a negative marker, but we have been unable to find a CRH antiserum that works in mouse brain and sought another immunofluorescence marker to positively identify Bar neurons for applications requiring counting or labeling Bar neurons after lesions and other manipulations in mice with a genetic background other than a GFP reporter for CRH. Like most brain regions, the pontine tegmentum contains many neurons immunoreactive for NeuN (Fox3), admixed with many unlabeled neurons. We found prominent NeuN labeling in a cluster of neurons medial to the LC, in the same location as the core of Bar (Figure 3), but neither the LC nor a prominent arc of cells along the ventromedial rim of Bar (dashed outline in Figure 3a) were labeled. The presence of NeuN in Bar, combined with the absence of NeuN in these two flanking regions makes it a practical marker for identifying the core of Bar in fluorescence preparations when combined with TH labeling as shown here.

3.3 *Vglut2*-glutmatergic and *Vgat*-GABAergic neurons in and around Bar

Again labeling for TH to localize LC as a landmark, we compared the distribution of a GFP reporter for the excitatory neuron marker *Vglut2* (Vglut2-IRES-Cre; R26-lsl-L10-GFP) or the inhibitory neuron marker Vgat (*Vgat-IRES-Cre; R26-lsl-L10-GFP*). Outside Bar, we found robust expression of these reporters in established glutamatergic populations including the parabrachial nucleus (*Vglut2*+), or in well-known GABAergic neurons including Purkinje cells in the cerebellum (*Vgat*+).

Bar contained densely packed neurons expressing the GFP reporter for *Vglut2* (Figure 4a), suggesting that most Bar neurons are glutamatergic. Interestingly, many LC neurons express this GFP as well. In contrast to the ubiquitous *Vglut2* reporter labeling in the core of Bar, virtually none of its neurons express a GFP reporter for *Vgat* (Figure 4b). This indicates that from embryonic development through adulthood, Bar neurons never assume an GABAergic or glycinergic fast-neurotransmitter identity. Similarly, LC neurons do not express *Vgat* reporter and the combined Bar plus LC forms a prominent void, surrounded by many GFP-expressing neurons; TH immunofluorescence in *Vgat* reporter mice tissue restricted this overall void to a shape, size, and location matching the core of Bar (Figure 4b). Within Bar, there are very few, small GFP-expressing neurons, greatly outnumbered by neurons reporting *Crh* or *Vglut2* in the reporter mice shown above. Medial and ventral to Bar, we found a dense population of small, putatively GABAergic neurons in the pontine central gray matter (PCG) having approximately the same size and distribution as the NeuN-poor region highlighted in Figure 3a.

3.4 Rostrocaudal distribution of cholinergic, catecholaminergic, and glutamatergic neurons

Again using a GFP reporter for *Vglut2* (*Vglut2-IRES-Cre; R26-lsl-L10-GFP*), we examined the rostrocaudal distribution of multiple neuronal populations in and around Bar (Figure 5). First, the dense population of *Vglut2*-reporting neurons in the core of Bar extends rostrally and caudally (Figure 5c–e) into all regions containing Bar^{CRH} GFP reporter shown above. Next, we clarified the distribution of cholinergic neurons in the LDT due to previous studies suggesting that the anatomic substrate for PMC function is the “nucleus tegmentalis laterodorsalis” (TLD) (Hida & Shimizu, 1982; Loewy et al., 1979; Satoh, Shimizu,

Tohyama, & Maeda, 1978). We identified LDT neurons by immunofluorescence labeling for choline acetyltransferase (ChAT) and found them distributed dorsally, medially, and rostrally outside Bar and separate from the LC.

Unexpectedly, many ChAT-immunoreactive neurons in the LDT and TH-immunoreactive neurons in the LC also express GFP, indicating that they (or a developmental precursor) had expressed *Vglut2* at one time. We did not find any neurons expressing both ChAT and TH. The densely packed, GFP-expressing neurons in the core of Bar are not as large or as distinctive as neurons in either LC or LDT, and none of them are immunoreactive for ChAT or TH. Similarly, in GFP reporter mice (*Crh-IRES-Cre; R26-lsl-L10-GFP)*, no Bar^{CRH} neurons contained ChAT or TH immunofluorescence, nor did we find any double-labeling for ChAT or TH in Bar^{CRH} neurons labeled by adult, Cre-conditional expression of other fluorescent proteins (below). Thus, Bar/Bar^{CRH}, LC, and LDT are entirely separate populations in the mouse tegmentum.

3.5 FoxP2 neurons surround Bar

We identified two additional populations surrounding Bar. One is glutamatergic, and the other, GABAergic, and both contain small neurons distinguished from surrounding populations by their nuclear immunoreactivity for the transcription factor FoxP2 (Figure 6).

The first population, glutamatergic FoxP2 neurons, divides the dorsolateral Bar core from the dorsal LC, filling the dashed outline from Figure 2d. In these neurons, nuclear immunoreactivity for FoxP2 colocalizes with a GFP reporter for *Vglut2* (Figure 6a–c), but not *Vgat* (Figure 6d–f). These FoxP2/*Vglut2* neurons distribute laterally and slightly caudally to Bar, extending through the LC and mesencephalic trigeminal nucleus (Me5) and into medial parabrachial nucleus (PB). This tangle of neurons is homologous to the rat "pre-LC" (Geerling & Loewy, 2007; Geerling et al., 2011). In rats, pre-LC neurons form a tight cluster immediately rostral to the LC, while in mice their distribution is more complex. We adopted the simpler abbreviation used by Garfield et al., "pLC" (Garfield et al., 2015).

The second population, GABAergic FoxP2 neurons, runs along the ventromedial aspect of Bar, occupying the NeuN-poor zone outlined in Figure 3a. Its neurons contain nuclear immunoreactivity for FoxP2, lack *Vglut2* reporter (Figure 6a–c), and express *Vgat* reporter (Figure 6d–f). We are not aware of any nomenclature or other information pertaining to these neurons in any species, so for now we refer to this population simply as "FoxP2/*Vgat*."

3.6 Developmental origin

Math1/*Atoh1*, a transcription factor expressed in the rhombic lip during embryogenesis, is required for the development of cerebellar granule cells as well as several brainstem populations, including Bar^{CRH} neurons (Rose, Ahmad, Thaller, & Zoghbi, 2009). To confirm this, we examined available tissue from P0 Cre-reporter mice for *Math1/Atoh1* (*Atoh1-Cre; R26-lsl-YFP*), in which YFP expression marks the mitotic progeny of any cells expressing the transcription factor *Math1*/*Atoh1* during embyrogenesis (Gray, 2008). At birth, (P0) the pontine tegmentum contained a discrete cluster of YFP-expressing (*Math1*/*Atoh1*-derived) neurons resembling the core of Bar (Figure 7). As in adult mice, these neurons in the core of Bar are surrounded by two populations of neurons with FoxP2-

immunoreactive nuclei: (1) dorsolateral FoxP2 neurons (pLC), which are also *Math1*/*Atoh1*-derived (express YFP), and (2) ventromedial FoxP2 neurons, which lack YFP. The LC also lacks YFP, consistent with its separate developmental origin from precursors expressing *Phox2a*/*Phox2b* (Morin et al., 1997; Pattyn, Goridis, & Brunet, 2000).

3.7 Dendritic arbors

Neurons typically receive most excitatory synapses on their dendrites, yet no previous studies of Bar neurons have labeled the full extent of their dendrites. To do this, we expressed in Bar^{CRH} neurons a red fluorescent protein that is membrane-targeted and Cre-conditional (Figure 8). Injecting AAV-hSyn-DIO-hM3D(Gq)-mCherry into the pontine tegmentum of *Crh-IRES-Cre* mice ($n = 6$) transduced neuronal somata in a highly restricted zone primarily within the core of Bar (white dots, Figure 8e–g), similar to the distribution of Bar^{CRH} neurons shown above. As in L10-GFP reporter mice, Bar^{CRH} neurons labeled by this Cre-conditional approach in adult mice do not express TH or ChAT.

"Native" fluorescence from mCherry itself is bright enough to see cell bodies and some proximal dendrites, but immunofluorescence labeling for mCherry reveals membrane labeling of dendrites extending ~0.5 mm dorsal and rostral-ventral to Bar, as well as faint labeling in thin axonal processes extending several millimeters away from Bar into the reticular formation (dorsal to the superior olive and facial nucleus) or into the periaqueductal gray. Axonal labeling with this approach was difficult to discriminate from background fluorescence, and was less consistent across cases, in contrast to the bright, consistent labeling in dendrites. Dendrites are thicker and more brightly labeled and end abruptly without forming en passant or terminal boutons, while axons are thinner, lighter, more variably labeled, form boutons, and arborize extensively in their terminal fields. To emphasize the thicker, brighter labeling in dendrites, we adjusted the contrast in Figure 8, obscuring the faint labeling in axons.

In the case shown in Figure 8, as in other cases with hM3D(Gq)-mCherry expressed in Bar^{CRH} neurons ($n = 6$ total), and both cases with ChR2-mCherry ($n = 2$, described below), mCherry immunoreactivity revealed thick, bright dendrites. These dendrites extend far beyond the recognized borders of Bar (Dong and The Allen Institute for Brain Science, 2008; Paxinos & Franklin, 2008) and beyond even what we anticipated from CRH immunolabeling in rats (Rouzade-Dominguez et al., 2003) or retrograde protein labeling from the spinal cord (Rizvi et al., 1994).

The most prominent Bar^{CRH} dendrites form a bundle extending rostrally and ventromedially, along and through the ventral cholinergic neurons in LDT (sublaterodorsal region, SLD) and into the midbrain reticular formation. These Bar^{CRH} dendrites continue rostrally past the merger of LDT with the pedunculopontine tegmental nucleus (PPN), then terminate abruptly. The longest dendritic branches (arrows in Figure 8b–f) terminate 500–600 μm rostral to Bar without branching or forming terminal boutons as would axons. The second most prominent bundle of Bar^{CRH} dendrites extends directly up to the fourth ventricle (4V). The tips of these branches cover a roughly 400 μm-wide patch along the rostral, lateral corner of the 4V. These dorsal dendrites occupy a volume of cell-poor tissue above Bar that is at least as large as the core of Bar. A third major bundle of dendrites (Figure 8h) extends

caudally into a space behind Bar that is almost as large as the core of Bar, overlapping the medial dendritic arbors of LC neurons (see Figures 2f and 3b and intermingling with the caudal extent of FoxP2/*Vglut2* (pLC) neurons.

3.8 Axonal projections to the spinal cord

Next, to characterize the axonal projections from Bar^{CRH} neurons to the lumbosacral spinal cord, we used Cre-conditional ChR2-mCherry, which traffics more avidly into axons than hM3Dq-mCherry. Injecting AAV-DIO-ChR2-mCherry into the pontine tegmentum of *Crh-IRES-Cre; Chat-GFP* mice ($n = 2$) allowed us to label the axons of many Cre-expressing Bar^{CRH} neurons while visualizing GFP labeling in cholinergic neurons (Tallini et al., 2006). In these cases, slightly larger AAV injection volumes resulted in a small number of labeled neurons outside Bar. These were found caudally, in the medial vestibular nucleus, and ventrolaterally, between the caudal parabrachial and principal sensory trigeminal nuclei. Neither case contained any neurons labeled in the LC or LDT, but due to this spread of AAV resulting in ChR2-mCherry expression in some CRH neurons outside Bar, we do not consider the full distribution of axonal labeling throughout the brain to be entirely specific to Bar^{CRH} axons and instead focused on axonal labeling in the lumbosacral spinal cord, where axonal projections from the pontine tegmentum originate exclusively from Bar and LC (Loewy et al., 1979; Rizvi et al., 1994; Satoh, Tohyama, et al., 1978; VanderHorst & Ulfhake, 2006; Valentino et al., 1994).

Axons labeled with ChR2-mCherry project ventrally from Bar, skirt the medial boarder of the motor trigeminal nucleus, and continue caudally into the lateral medullary reticular formation. Many of these axons ramify in the ventral reticular formation, just above the dorsal surface of the superior olivary nucleus or facial motor nuclei. A combination of arborizing and long axonal projections continues caudally through the entire reticular formation of the ventrolateral medulla and reach the lateral column (aka lateral funiculus) of the ipsilateral spinal cord, where a dense cluster of labeled axons runs the full length of the spinal cord.

At all spinal levels, one or a few axonal branches ramify sparsely in the central gray matter or in the vicinity of the lateral spinal nucleus, but we found concentrated branching and boutons only in the lumbosacral region (Figure 9b–g). There, labeled axons ramify extensively, forming a horizontal streak across the spinal gray matter. Clusters of boutons envelop most or all of the autonomic preganglionic neurons in the sacral intermediolateral nuclei bilaterally (IML, cholinergic, GFP+ in Figure 9h,i). Centrally, primarily at low lumbar and uppermost sacral levels (L5/6 to S1/2), Bar^{CRH} axons branch into a broad, dense terminal field. This dense terminal field fills the expanded central gray matter beneath the dorsal columns at these levels, which is known as the dorsal gray commissure (DGC, Figure 9h) or dorsal commissural nucleus (DCN) (Blok, de Weerd, & Holstege, 1997; Fowler, Griffiths, & de Groat, 2008). Spinal regions outside the DGC/DCN and IML receive sparse or no axonal labeling. One or a few axons extend from the lateral funiculus into deep laminae of the ventral horn or along the lateral part of lamina I at all levels of the spinal cord, even at caudal coccygeal levels, but we do not find any dense or prominent terminal fields in the ventral horn at any level, and specifically not in the lumbosacral “dorsolateral

nucleus," the rodent equivalent of Onuf's nucleus, which contains somatic motoneurons that innervate the external urethral sphincter (McKenna & Nadelhaft, 1986).

Complementing our anterograde labeling, we next injected a CTb, a retrograde tracer into the upper sacral spinal cord (Figure 10) to characterize the identity and distribution of any neurons in the pontine tegmentum that project axons to this level. We made these injections in CRH reporter mice ($n = 2$ *Crh-IRES-Cre; R26-lsl-L10-GFP*) and immuno-labeled TH to compare retrograde labeling in Bar and LC. As expected from previous work in rats, virtually all the retrogradely labeled neurons in the pontine tegmentum were found in either Bar or LC. Retrogradely labeled LC neurons contain TH (pink in Figure 10a). These spinally projecting neurons were clustered primarily in the ventral LC, with fewer neurons scattered in the reticular formation ventral to it, in a region referred to in rats and cats as "subcoeruleus" or "subcoeruleus alpha." Outside the LC and subcoeruleus, spinally projecting neurons in the tegmentum cluster exclusively in Bar and lack TH. The majority express GFP (orange-yellow in Figure 10), representing between 50 and 70% of all noncatecholaminergic CTb-labeled neurons. A minority of retrogradely labeled neurons in Bar lacked GFP in both cases (red in Figure 10). Control injections into the mid-thoracic spinal cord produced the same pattern of retrograde labeling in a smaller number of tegmental neurons, with a larger proportion of LC/subcoeruleus catecholamine neurons and relatively few neurons in Bar.

4 DISCUSSION

After clarifying the location and distribution of Bar^{CRH} neurons in mice, we identified markers for at least five separate populations of neurons surrounding Bar (Figure 11a). Our most important new finding is that Bar^{CRH} dendritic arbors are unexpectedly massive (Figure 11b), and thus may receive synaptic input from a broader range of afferent neurons than were identified in experiments focusing on the core of Bar. The neuroanatomic framework provided here will improve the interpretation of cell type-specific experiments in this region, which can characterize the specific populations of neurons involved in specific pelvic functions, including bladder contraction and urethral sphincter relaxation.

This region of the brainstem suffers from the divergent terminology of different groups working in different animal species over the past century. To help resolve past debate and confusion, here we review the neuroanatomy and nomenclature of the PMC region, as well as Bar^{CRH} projections to the spinal cord and implications of our new finding that their dendritic arbors extend well outside the core of Bar.

4.1 Basic nomenclature

The terminology involving neurons in the pontine tegmentum is unnecessarily complex and inconsistent. The neurons now called Barrington's nucleus were identified in rats in the late 1970s (Loewy et al., 1979; Satoh, Tohyama, et al., 1978; Tohyama et al., 1978). Two groups of investigators showed that these neurons survive treatment with 6-hydroxydopamine and are therefore separate from the LC, and each group proposed that they were Barrington's "micturition reflex center," with Loewy et al. coining the term "pontine micturition center." Both groups also used the Latin term "nucleus tegmentalis laterodorsalis" (TLD) for their

neuroanatomical location, but this term is no longer used. “TLD” initially referred to a larger region of the pontine tegmentum (Castaldi, 1926) until Saper, Scammell, and Lu (2005) co-opted and Anglicized the term to “laterodorsal tegmental nucleus” (LDT), referring selectively to cholinergic neurons here (Armstrong, Saper, Levey, Wainer, & Terry, 1983). LDT is now the accepted name for this cholinergic population (Paxinos & Franklin, 2008; Paxinos & Watson, 2006), which is entirely separate from Bar.

At the same time, Tohyama et al. introduced the term “BARRINGTON nucleus,” and used this term interchangeably with “TLD” (Tohyama et al., 1978). Saper and colleagues (2005) adapted this to the possessive form “Barrington’s nucleus” (Standaert et al., 1986), which now is used in all major brain atlases (Swanson, 2004; Paxinos & Watson, 2006; Dong and The Allen Institute for Brain Science, 2008; Paxinos & Franklin, 2008). We prefer this to “PMC” because PMC refers to a functional “center” rather than a specific population of neurons and has been applied with varying degrees of specificity in the past, referring sometimes to Bar, sometimes to a larger region that includes Bar, and sometimes even to neurons well outside Bar (Noto et al., 1991). Bar is a neuroanatomically defined population of neurons, which may participate in micturition and possibly other functions, while PMC refers less specifically to a functional hypothesis about this region and incorporates an as-yet unsubstantiated assumption that neurons here function primarily or exclusively in micturition. Despite some evidence that Bar^{CRH} neurons are involved in PMC function (Hou et al., 2016), there may not be a simple, one-to-one relationship between Bar (or Bar^{CRH}) neurons and the older term “PMC.” In fact, Bar^{CRH} neurons are activated equally by distending the distal colon or bladder (Rouzade-Dominguez et al., 2003), appear to innervate all pelvic visceral motoneurons in the sacral IML (above), and may modulate pelvic functions beyond just micturition (Holstege, 2016).

Confusing and contradictory terminology in this region extends outside Bar as well. For example, stimulation sites in the rat PAG (dorsal and rostral to Bar), were both referred to as the “pontine micturition center” and labeled “LDT” in the same study rat study (Noto, Roppolo, Steers, & de Groat, 1989), and PMC function in both rats and cats has been attributed to neurons in the LDT, LC, or the subcoeruleus region (Kuru, 1965; Kuru & Yamamoto, 1964; Mallory et al., 1991; Nishizawa et al., 1988; Noto et al., 1991; Satoh, Shimizu, et al., 1978; Sugaya et al., 1987).

It is our hope that this background information, combined with new neuroanatomic data will promote a consistent and precise terminology for neurons in and around Bar, at least in rodents. In other species, more work is needed. In cats, Holstege and colleagues identified a homologous spinally projecting population, rostral and ventromedial to the LC (Holstege et al., 1986), which they named the “M-region.” Yet even in this species—the primary source of micturition physiology beginning with Barrington in the early 20th century (Barrington, 1927; Kabat, Magoun, & Ranson, 1936; Tang, 1955)—we lack basic information about gene and protein markers, including CRH. In humans, non-human primates, and other species we know even less (Blanco et al., 2013).

4.2 Bar development, *Crh* expression, and neurotransmitters

By late embyrogenesis, *Crh*-expressing cells appears in the vicinity of Bar (see in situ hybridization labeling for *Crh* in the mouse brainstem at E18.5, image 12 from the Allen Brain Institute; developingmouse.brain-map.org). These *Crh*-expressing neurons originate from *Math1*/*Atoh1* –expressing precursors in the rhombic lip neuroepithilium, then migrate to their adult positions before birth. These conclusions are based on the identification of *Math1*/*Atoh1*-derived neurons in this same *Crh*-expressing region in E18 embryos by Rose et al. (2009), who also showed that *Crh*-expressing neurons fail to appear here in *Math1*/*Atoh1*-knockout mice. Now, using a Cre-reporter in early-postnatal mice, we confirm that Bar neurons derive from *Math1*/*Atoh1*-expressing precursors. *Math1/Atoh1*-derived neurons fill the entire core of Bar, so it is likely that all Bar neurons share this embyronic origin, whether or not they express CRH.

CRH peptide in Bar was first identified in the adult rat brainstem using immunohistochemistry after i.c.v. treatment with colchicine. The initial report mentioned the presence of CRH-immunoreactive neurons “in the LDT and in a restricted zone in the ventral half of the locus coeruleus” without comparing markers for LDT or LC neurons (Swanson et al., 1983). The following year, Vincent and Satoh co-localized CRH immunoreactivity in neurons retrogradely labeled by injecting a tracer into the spinal cord, but they presented just one high-magnification image without showing the anatomic location or referring to the population by name (Vincent & Satoh, 1984).

Later, *Crh* mRNA was labeled by in situ hybridization (Imaki et al., 1991) and subsequent investigators confirmed that a subset of spinally-projecting Bar neurons are immunoreactive for the neuropeptide (Rizvi et al., 1994; Rouzade-Dominguez et al., 2003; Valentino et al., 1994), so CRH became a de factor marker for Bar in rats. The number and distribution of CRH-immunoreactive, spinally-projecting neurons in rats was described best by Valentino and colleagues (Valentino et al., 1994, 1995), who found that CRH immunoreactivity (after colchicine) and retrograde tracing from the spinal cord label neurons outside the core of Bar in a more extensive distribution, which was indistinct in Nissl preparations. In that respect, mice are similar to rats, and the main species difference we identified is that Bar^{CRH} neurons are co-extensive with the LC in mice, while in rats they are rostral to the LC.

Immunolabeling CRH in this region typically requires pre-treatment with colchicine, which interrupts axonal transport to boost the concentration of neuropeptide in the cell body, and, incidentally, causes severe urinary retention (Zanoli & Ferrari, 1988). Thus far, even after colchicine treatment we have not had good results immunolabeling CRH in mice. To our knowledge, two previous groups have claimed to label Bar^{CRH} neurons in mice after colchicine treatment; one did not show any images (Wang et al., 2011), and the other presenting an image with immunoreactivity in punctae, not cell bodies (Blanco et al., 2013). Even if we were to identify an antiserum or tissue protocol to immunolabel CRH in mice, preinjecting a neurotoxin is impractical for routine histologic assays and would not allow us to identify living Bar^{CRH} neurons for in vivo calcium imaging or slice electrophysiology.

Fortunately, the CRH Cre-reporter mouse circumvents these limitations. The efficiency of Cre-reporters is sometimes less than ideal (Liu et al., 2013) and it is possible that not every

Bar^{CRH} neuron produces GFP, but in our experience labeling in this strain is consistent litter to litter, across age and gender. Our report provides a roadmap to the location and distribution of neurons accessible in physiology experiments using *Crh-IRES-Cre* mice to target Bar^{CRH} neurons, which was the primary goal of this study (see also Hou et al., 2016).

There is a close correspondence between the expression of Cre-reporter and *Crh* mRNA in adult Bar neurons. This was shown recently by Hou et al., who identified *Crh* expression in 90% of Cre-expressing in adult *Crh-IRES-Cre* mice (Hou et al., 2016). These investigators estimated that 44% of PMC neurons contain *Crh* mRNA (Hou et al., 2016), similar to Valentino's report in rats that 50% of the Nissl-stained Bar neurons were CRH-immunoreactive after colchicine treatment (Valentino et al., 1995). Here, due to the nontrivial geometry of Bar and surrounding neurons and the lack of a marker specific to its non-CRH neurons, we used retrograde labeling from the spinal cord to label the full population. This approach circumvents the possibility of including Bar neurons that project to the forebrain or brainstem rather than the spinal cord (Valentino et al., 1995), though an individual tracer injection may not label all spinally projecting Bar neurons. Using this approach, we estimate that slightly more than half the spinal-projecting neurons in Bar produce CRH. Thus, a sizeable subpopulation of spinal-projecting Bar neurons lack CRH. It remains to be determined whether the non-CRH subset mediates a different function than Bar^{CRH} and which markers for neurons in this region, such as estrogen receptor alpha (VanderHorst et al., 2005) may identify them.

Regarding the function of CRH itself, beyond its value as a histochemical marker, there is no direct evidence that Bar neurons release this neuropeptide from their synaptic terminals in the spinal cord. Assuming this does occur, it remains unclear whether and how CRH influences spinal neurons. *Crh*-knockout mice have been available for more than two decades (Muglia, Jacobson, Dikkes, & Majzoub, 1995), but no published reports have mentioned urinary bladder or voiding abnormalities. Mice with global *over*expression of *Crh* do voided more frequently (Million et al., 2007), yet overexpressing *Crh* in and around Bar prolonged inter-void latency in rats (McFadden, Griffin, Levy, Wolfe, & Valentino, 2012). In anesthetized rats, injecting CRH peptide into the spinal cord mildly inhibited voiding in one laboratory (Kiddoo et al., 2006; Pavcovich & Valentino, 1995) and produced somewhat different effects in another (Klausner et al., 2005). Intrathecal injection of receptor antagonists induced urinary frequency (Kiddoo et al., 2006; McFadden et al., 2012; Pavcovich & Valentino, 1995), though the site of action remains unclear because similar results were found after systemic administration (Kiddoo et al., 2006). To our knowledge, micturition itself has not been tested in receptor-knockout mice, though one study identified CRFR2 expression in the bladder wall and a CRFR2-dependent mechanism for bladder inflammation by acute stress (Boucher, Kempuraj, Michaelian, & Theoharides, 2010).

In contrast to the lack of clarity regarding peptidergic co-transmission, there is good evidence that glutamate is a fast-synaptic neurotransmitter for Bar/PMC neurons in mice, rats, and cats. *Vglut2* mRNA expression is prominent in Bar in adult rats (Stornetta, Sevigny, & Guyenet, 2002) and was found in 94% of *Crh*-expressing neurons here in mice (Hou et al., 2016), consistent with the ubiquitous *Vglut2* GFP reporter labeling shown here. Further, voids triggered by electrically stimulating the PMC can be abolished by injecting

glutamatergic antagonists into the spinal cord (Matsumoto, Hisamitsu, & de Groat, 1995; Yoshiyama, Roppolo, & de Groat, 1995).

4.3 Surrounding populations

At least five populations of neurons surround Bar (Figure 11a), including neurons identified here for the first time. Me5 neurons' straightforward connections and function as proprioceptors to muscles of mastication are discussed elsewhere (Pang et al., 2006), but the other four populations merit further consideration.

4.3.1 Pontine central gray—Medial to Bar, the PCG contains many GABAergic neurons (*Vgat*-reporting), and sparse glutamatergic neurons. Along the ventromedial surface of Bar is a specific subpopulation of PCG neurons expressing both *Vgat* and FoxP2 (Figure 6). Unlike FoxP2 neurons in PB, pLC, and Bar, these GABAergic neurons do not derive from *Math1*/*Atoh1* precursors (Figure 7). Instead, they may derive from *Ptf1a* precursors in the ventricular zone, which give rise to all GABAergic neurons in the cerebellum, and some in the hindbrain (Fujiyama et al., 2009; Gray, 2008; Hoshino et al., 2005; Yamada et al., 2014). Whatever their origin, local inhibitory neurons may directly sculpt the activity of Bar^{CRH} neurons. Bar neurons are under GABAergic inhibitory control because dis-inhibiting the PMC region with bicuculline reduces the interval between voids by more than 50% (Mallory et al., 1991). At least some of the inhibitory input may derive from local neurons, and the spiking of units just outside Bar is inversely proportional to bladder pressure and Bar neuron firing (Koyama, Imada, Kawauchi, & Kayama, 1999; Tanaka et al., 2003). Targeting these neurons for stimulation and recordings in *FoxP2-* and *Vgat-IRES-Cre* mice would test the possibility that local interneurons in the PCG suppress the activity of Bar^{CRH} neurons during bladder filling, which could be a fundamentally important mechanism for urinary continence. This possibility would not preclude a role for other inhibitory afferents to Bar, for example in the periaqueductal gray or preoptic hypothalamus (Hou et al., 2016; Valentino et al., 1994).

4.3.2 Pre-locus coeruleus—Just dorsolateral to Bar, a small population of FoxP2-expressing, glutamatergic neurons forms the pLC. Like Bar and other hindbrain neurons, pLC neurons develop from *Math1*/*Atoh1* precursors in the rhombic lip. Mouse pLC neurons are homologous to the pre-LC in rats, which likewise express FoxP2 and are activated by dietary sodium deprivation via aldosterone-sensitive neural input (Geerling & Loewy, 2007; Geerling et al., 2011; Jarvie & Palmiter, 2017). Unlike rats, in which these neurons form a discrete cluster rostral to the LC, the pLC in mice wraps around LC and even extends through Me5 and into the medial PB. In mice, without markers for Bar and LC, the lateral and medial parts of the pLC population may be mistaken for neurons in PB, Bar, or LC (see Supplementary figure 9b in Jarvie & Palmiter, 2017). Besides FoxP2 and *Vglut2*, pLC neurons do not express most other markers we tested, including *Vgat*, CGRP, CCK, Lmx1b, TH, and ChAT, but a small subset do express *Pdyn* (Geerling et al., 2016). Based what is known about their input-output connections (Geerling & Loewy, 2006; Geerling, Shin, Chimenti, & Loewy, 2010; Garfield et al., 2015; Shin, Geerling, Stein, Miller, & Loewy, 2011), it is unlikely that pLC neurons regulate micturition, though their proximity to Bar

implies that they would have been affected in all "PMC" experiments using electrical stimulation, electrolytic lesions, or drug infusions.

4.3.3 Locus coeruleus—Immediately lateral to Bar lies one of the most well-known populations of neurons in the brainstem. Much has been written about the roles of these broadly projecting, noradrenergic neurons in arousal, stress, autonomic function, cognition, and behavior (Aston-Jones & Waterhouse, 2016; Bruinstroop et al., 2012; Carter et al., 2010; Gompf et al., 2010; Morin et al., 1997). The proximity between Bar and the LC has long tempted speculation that one somehow supplies the other with information related to stress, arousal, or visceral state. Neuroanatomic and pharmacologic data support the idea that LC neurons may communicate stress-related signals to Bar^{CRH}, or that Bar^{CRH} neurons release CRH onto LC neurons as part of stress responses (Curtis, Lechner, Pavcovich, & Valentino, 1997). Now, with Cre mice available for selectively targeting either population, these hypotheses can be tested directly. Electrophysiologic data vary as to whether LC neurons increase their activity in association with bladder pressure and voiding, with some investigators claiming an association (Koyama, Imada, Kayama, Kawauchi, & Watanabe, 1998; Page, Akaoka, Aston-Jones, & Valentino, 1992) and others finding none (Tanaka et al., 2003). Ventral LC and subcoeruleus neurons project many axons to the lumbosacral spinal cord in both rats (Loewy et al., 1979; Satoh, Tohyama, et al., 1978; Tohyama et al., 1978) and mice (VanderHorst & Ulfhake, 2006), and the presence of adrenergic signaling from LC to the spinal cord may be necessary for the voiding reflex (Yoshimura, Sasa, Yoshida, & Takaori, 1990), yet focally stimulating LC with small currents does not trigger voiding (Yamao et al., 2001) and focal, bilateral lesions centered in the LC in rats caused minimal or no urinary retention in rats (Satoh, Shimizu, et al., 1978). One caveat to the conclusion that LC neurons are somehow involved in voiding is that LC axons project indiscriminately to almost every part of the central nervous system, including most regions of the spinal cord. In the lumbosacral spinal cord, these axons ramify diffusely across the gray matter (Bruinstroop et al., 2012), with relatively few varicosities in the micturition-associated regions (DCG and IML) and relatively more in the dorsal horn, contrasting sharply with the projection pattern of Bar^{CRH} neurons. So if LC neurons do influence micturition, they likely do so indirectly, by modulating bladder sensory neurons in the dorsal horn, sphincter motoneurons in the ventral horn, or possibly even Bar^{CRH} neurons in the pons, and this probably occurs in the context of its broader LC modulation of sensory-motor functions, with a wide repertoire of effects at multiple spinal levels.

4.3.4 Laterodorsal tegmental nucleus—Rostral and dorsomedial to Bar is a prominent population of medium-large cholinergic neurons (Armstrong et al., 1983). In addition to cholinergic markers, LDT neurons express *Nos1* (nitric oxide synthase), and some investigators have identified these neurons using NADPH diaphorase histochemistry (Koyama et al., 1999; Rizvi et al., 1994). In rats, caudal LDT neurons arc medially over and through Bar (Rizvi et al., 1994), but in mice these two populations (LDT and Bar^{CRH}) are spatially segregated—no LDT neurons cross into or through Bar. Despite previous suggestions (Noto et al., 1991) and evidence that bladder stretch may influence the activity of some LDT neurons (Koyama et al., 1999), the LDT is no longer thought to play a role in micturition. LDT axons project rostrally, to the anterodorsal and other thalamic nuclei

(Hallanger, Levey, Lee, Rye, & Wainer, 1987), and are thought to be involved in forebrain functions possibly including arousal and REM sleep (Saper et al., 2005).

4.4 Dendritic arbors

The dendrites of Bar^{CRH} neurons, as revealed by Cre-dependent expression of two different mCherry-containing vectors, are extensive. They extend in several directions much further than the maximum diameter of the core of Bar. Previous studies used immunolabeling for CRH (Peoples, Wessendorf, Pierce, & Van Bockstaele, 2002), juxtacellular filling of Bar neurons with neurobiotin (Rouzade-Dominguez et al., 2003), or retrograde tracing from the spinal cord (Loewy et al., 1979; Valentino et al., 1994) to visualize Bar dendrites in rats, but none of these techniques label them fully. We are not aware of any Golgi or other dendritic labeling approaches in any species, and could not find published data on this topic in mice.

The critical implication of a larger-than-expected dendritic arbor is that a Bar^{CRH} neuron probably collects and integrates many input connections outside the core of Bar, well beyond the region traditionally considered to involve Bar or micturition. Based on the trajectories of Bar^{CRH} dendrites overlapping other neuronal populations, such as the LDT, SLD, and LC, afferents to these regions should be reconsidered as potential afferents to Bar. Historically, anchoring bias has led to claims that axons terminating in this region target one of these more famous populations, most commonly the LC, when most or all of the axons in fact target neurons in Bar or pLC (Ennis, Behbehani, Shipley, Van Bockstaele, & Aston-Jones, 1991; Geerling et al., 2010).

The most detailed work on Bar afferents to date was performed by Valentino et al. who identified input from the ventrolateral PAG, lateral hypothalamic area, and preoptic area in rats (Valentino et al., 1994). Retrograde tracer injections into the core of Bar were followed by anterograde tracing in putative afferent sites to identify brain regions contributing axons to the core (Valentino et al., 1994). Based on the expansive dendritic arbors shown here, these experiments probably failed to identify afferent brain regions that project axons primarily (or exclusively) to Bar distal dendrites. For example, several cortical regions project axons into to the sublaterodorsal region of the reticular formation in the midbrain tegmentum beneath LDT (Boissard, Fort, Gervasoni, Barbagli, & Luppi, 2003), which contains a prominent rostral bundle of Bar^{CRH} dendrites. Cortical input to rostral Bar^{CRH} dendrites may underlie deliberate, contextually appropriate voiding. Hypothalamic and other subcortical neurons may target the caudal Bar^{CRH} dendrites in a region also containing LC dendrites, and still others probably synapse on the plume of dendrites extending dorsally from Bar to the fourth ventricle.

The existence of these large and discretely organized bundles of Bar^{CRH} dendrites should prompt a fresh evaluation of synaptic afferents to Bar^{CRH} dendrites relative to other tegmental neurons. Candidate afferents can be identified using a molecular approach with pseudotyped, G-deleted rabies virus, which is retrogradely transported from Cre-expressing neurons (Wickersham et al., 2007), and this technique indeed labeled cortical and other, unexpected candidate afferents in *Crh-IRES-Cre* mice (Hou et al., 2016). These candidate afferents now can be tested with optogenetic terminal stimulation and inhibition to test for synaptic connectivity and physiologic effects on awake-behaving micturition.

4.5 Axonal projections to the sacral spinal cord

Long before Cre-conditional Bar^{CRH} tracing in mice, anterograde tracing established that neurons here project to the sacral spinal cord in rats and cats (Holstege et al., 1986; Loewy et al., 1979), and retrograde tracing in rats revealed that many of these neurons contain CRH (Rizvi et al., 1994; Valentino et al., 1994; Vincent & Satoh, 1984). Our Cre-conditional axon tracing, and another recent report (Hou et al., 2016) verify these classic findings in mice, confirming that CRH-expressing neurons provide a substantial proportion of the overall Bar axonal projection to micturition-associated regions of the spinal cord.

Using this highly sensitive technique, we also observed light axonal labeling in the central gray and lateral dorsal horn at every level of the spinal cord. This is a novel finding, and raises new questions. Are Bar^{CRH} axons synapsing outside the lumbosacral regions branches of axons that also project to the lumbosacral region? And do they contribute to micturition-associated functions at all? Micturition is associated with a brief change in posture in most mammals, and in humans it incurs a slight predisposition towards fainting, which when it occurs is known as “micturition syncope” (Proudfit & Forteza, 1959). Perhaps the light, diffuse projection of Bar^{CRH} axons throughout the spinal central gray, above the lumbosacral region, modulates postural and/or sympathetic tone in parallel with the act of voiding itself. Alternatively, Bar^{CRH} terminations in the lumbosacral region or elsewhere may play a role in pelvic organ functions unrelated to micturition (Holstege, 2016; Rouzade-Dominguez et al., 2003).

Our retrograde tracing confirms in mice that spinally projecting, noncatecholamine neurons in the PMC region are clustered entirely in and around Bar and, based on their Cre-reporter expression, slightly more than half of these express CRH. As discussed above, our data add support to existing evidence for the existence of at least two Bar subpopulations: one expressing both *Crh* and *Vglut2*, and another with just *Vglut2*. Without a marker or Cre line specific for this non-CRH sub-population of Bar neurons, we cannot comment on any difference (or lack thereof) in its axonal projection pattern to the spinal cord or other sites. Microstimulation in and around Bar in rats identified roughly equal proportions of sites that trigger bladder contraction versus a combination of bladder contraction and sphincter relaxation, with a small number of sites producing sphincter relaxation alone (Yamao et al., 2001). It is of interest to gain genetic access to this non-CRH Bar subpopulation and test whether stimulating it vs. Bar^{CRH} neurons affects the bladder or sphincter or both. For example, optogenetic stimulation of Bar^{CRH} neurons causes detrusor contraction in anesthetized mice (Hou et al., 2016), but it remains unclear whether these neurons can trigger sphincter relaxation, which is necessary for voiding. Their dense Bar^{CRH} projection to both the DGC and the sacral IML suggests that they could synchronize sphincter relaxation (via DGC interneurons) and bladder contraction (via the IML), yet individual Bar^{CRH} neurons or the non-Bar^{CRH} subpopulation may influence the bladder or sphincter tone in isolation, and some Bar neurons likely participate in visceral pelvic functions unrelated to micturition (Holstege, 2016; Rouzade-Dominguez et al., 2003).

4.5.1 Pathways from Bar to bladder and sphincter—The pattern of Bar^{CRH} axonal terminations within the spinal gray matter is critical to current models of the neural control

of voiding. These models emphasize the hypothesis that branched projections from the PMC simultaneously excite neurons in the DGC and IML, which coordinates bladder contraction and relaxation of the external urethral sphincter, respectively, (Blok et al., 1997; Fowler et al., 2008). Coordinating these two activities—bladder contraction and sphincter relaxation—is the sine qua non of voiding, and its interruption by spinal injuries produces the clinical syndrome of *bladder-sphincter dyssynergia*, in which sphincter contraction is uninterrupted or even augmented, unhelpfully, during bladder contractions (Fowler, 1999; Sakakibara, 2015).

The multisynaptic pathway for bladder contraction appears straightforward: PMC neurons form excitatory-type synapses on cholinergic, preganglionic neurons in the sacral IML (Blok & Holstege, 1997), which in turn release acetylcholine onto cholinergic, postganglionic neurons along the bladder wall. Nicotinic receptor activation on these postganglionic neurons causes them to release acetylcholine in the detrusor muscle, activating M3 muscarinic receptors and causing contraction (Fowler et al., 2008).

For sphincter relaxation, however, the pathway is more complex. Motoneurons to the external urethral sphincter lie in a special region of the ventral horn called Onuf's nucleus in cats and primates or the "dorsolateral nucleus" in rodents (McKenna & Nadelhaft, 1986). Micro-stimulating this region in cats *tightens* the external urethral sphincter, as expected (Grill, Bhadra, & Wang, 1999), and the primary mechanism for maintaining sphincter tone is a spinal reflex by which bladder stretch increases the activity of Onuf's motor neurons (de Groat, Griffiths, & Yoshimura, 2015). Layered atop this reflex are descending pathways from the brainstem, which briefly cause a net inhibition when the bladder contracts. One way this is thought to occur is through Bar axon terminals stimulating GABA/glycine interneurons in the DGC, which then inhibit sphincter motoneurons in the ventral horn (Fowler et al., 2008). In support of this model, injecting pseudorabies virus into the external urethral sphincter produces a retrograde infection first of motorneurons in the dorsolateral nucleus, next of interneurons in the DGC, and later in Bar (Nadelhaft & Vera, 1996). Further, axons projecting from the cat homolog of Bar (the "M-region") form excitatory-type synapses with GABAergic and glycinergic interneurons in the DGC (Blok et al., 1997; Sie, Blok, de Weerd, & Holstege, 2001), and microstimulating the DGC phasically decreases sphincter tone (Blok, van Maarseveen, & Holstege, 1998; Grill et al., 1999).

4.5.2 Supraspinal Bar^{CRH} projections—In addition to projections to the spinal cord, Bar neurons also project axons to the brainstem and hypothalamus. Conventional anterograde and retrograde tracing in rats revealed axonal projections from CRH-immunoreactive neurons in Bar to the PAG, medial preoptic area, and dorsal motor nucleus of the vagus (Valentino et al., 1995). We found similar projections in mice after Cre-conditional labeling with ChR2-mCherry, but the labeling of CRH neurons outside Bar limits our ability to definitively interpret the origin of each projection to targets other than the lumbosacral spinal cord without additional retrograde and anterograde tracing experiments.

4.6 Limitations

Our data clarify several distinctions between Bar and surrounding populations, but certain limitations in our techniques and data merit consideration.

First, using a Cre-reporter is the most robust, practical way to identify Bar^{CRH} neurons, but this approach may leave some neurons unlabeled due to inherent inefficiencies with most Cre reporters (Liu et al., 2013). Finding an antibody that labels mouse CRH, or labeling *Crh* mRNA using fluorescence *in situ* hybridization could help clarify exactly what proportion of neurons expressing the GFP reporter also produce CRH (Hou et al., 2016), but as discussed above, defining the subpopulation of glutamatergic neurons that lack CRH in greater detail will require identifying another marker that more specifically distinguishes them than *Vglut2*, which is expressed in many neurons outside Bar.

Next, using a Cre-reporter to label adult neurons leaves open the possibility of a "lineage effect" where only embryonic precursors of a given neuron expressed the Cre-driver gene, yet their daughter cells continue producing the reporter (L10-GFP) permanently, even after they stop expressing the Cre-driver gene (*Crh*). A lineage effect probably explains our observation that many LC and LDT neurons express a reporter for *Vglut2*, even though they do not express *Vglut2* in adult rodents (Stornetta et al., 2002). Similarly, adult Me5 neurons express *Vglut1*, not *Vglut2* (Pang et al., 2006), yet every *Vglut2* reporter mouse contained robust GFP reporting in Me5, probably reflecting previous or intermittent expression, similar to pyramidal neurons in the cerebral cortex and hippocampus (Vong et al., 2011). In contrast, a "lineage effect" does not explain the reporters for *Vglut2* and *Crh* in most Bar neurons, for the following reasons. First, these neurons lack any history of *Vgat* expression, based on the lack of *Vgat* Cre-reporter as shown here. Second, Bar neurons do not express *Vglut1* mRNA (Pang et al., 2006) and prominently express *Vglut2* mRNA in adult rats (Stornetta et al., 2002) and mice (Lein et al., 2007). Third, Bar neurons express *Crh* mRNA in adult rats (Imaki et al., 1991) and mice (Lein et al., 2007), and other investigators have found a greater than 90% correspondence between *Crh* mRNA and a separate Cre-reporter for *Crh-IRES-Cre* (Hou et al., 2016). Fourth, after injecting two different FLEX/DIO vectors in this region in adult *Crh-IRES-Cre* mice, we found robust expression of Cre-conditional proteins, signifying on-going transcription of the *Crh* locus in adult neurons here.

Finally, our Cre-conditional labeling of Bar^{CRH} axonal projections to the spinal cord confirms that these neurons project to and ramify extensively within the DGC and IML, but does not prove or disprove synaptic connectivity to any particular type of spinal neuron. In the future, ChR2-assisted circuit mapping (Petreanu, Huber, Sobczyk, & Svoboda, 2007) can test the presence and type of synapses between Bar^{CRH} neurons and postsynaptic neurons in the spinal cord, which we expect will include cholinergic neurons in the IML (labeled with *Chat-GFP*, Figure 9) and inhibitory interneurons in the DGC, which can be identified using *Gad67-GFP* mice (Tamamaki et al., 2003). The supraspinal connectivity of Bar^{CRH} neurons remains unresolved, but smaller injections delivering synaptophysin-mCherry can produce more precise maps of Bar^{CRH} axons and boutons in spinal and supraspinal targets, extending information from conventional anterograde and retrograde tracing in rats (Valentino et al., 1995).

Ultimately, the goal is not simply to create a catalog of neuroanatomical data for its own sake. Our driving interest is to use cell type-specific techniques to test each population of neurons in and around Bar and their overall circuits for roles in bladder contraction, sphincter relaxation, other possible pelvic functions, and micturition-associated autonomic and behavioral changes including micturition syncope, arousal, and the awareness of bladder filling that is likely critical for urinary continence.

5 CONCLUSION

The anatomic and genetic data presented here serve as a roadmap for targeting Bar and surrounding neurons with cell-type-specific, recombinase-based techniques in mice. Cre-driver mice are now available for targeting neurons in Bar (*Crh-IRES-Cre; Vglut2-IRES-Cre*), LDT (*Chat-IRES-Cre; Nos1-Cre*), LC (*TH-IRES-Cre; Dbh-Cre*), pLC (*FoxP2-IRES-Cre*), and the PCG (*Vgat-IRES-Cre*), and combining any of these with a second recombinase and Boolean viral vectors (Fenno et al., 2014) could allow even more precise targeting. The distal dendrites of Bar^{CRH} neurons, and those of surrounding neurons probably receive synaptic inputs missed by conventional tracing techniques, which are now being identified (Hou et al., 2016). By manipulating the activity of these neurons and their afferent network using DREADDs and opsins, ablating them, recording their activity in vivo (Chen, Lin, Kuo, & Knight, 2015), measuring their activity and connectivity in vitro using optical voltage indicators (Hochbaum et al., 2014) and testing their synaptic connectivity with channelrhodopsin-based circuit mapping (Petreanu et al., 2007), we can emerge from a fog of neuroanatomic speculation and begin to design hypothesis-testing experiments that pin specific functions onto specific neuronal populations and connections.

Acknowledgments

We thank Brad Lowell for generous use of shared mouse lines and equipment, David Olsen (*Crh-IRES-Cre* mice and *R26-loxSTOPlox-L10-GFP* reporter mice) and Linh Vong (*Vglut2-* and *Vgat-IRES-Cre* mice). We especially acknowledge Arthur Loewy and Clif Saper for their advice and constructive criticisms of early drafts of this manuscript.

Funding information

Grant sponsors: NIH P20 DK103086 (MZ, AV), NIH R25 NS070682; T32 HL007901 (JG), NIH R01 NS079623 (VV), NIH RO1 HL089742 (PAG)

References

Armstrong DM, Saper CB, Levey AI, Wainer BH, Terry RD. Distribution of cholinergic neurons in rat brain: Demonstrated by the immunocytochemical localization of choline acetyltransferase. The Journal of Comparative Neurology. 1983; 216:53–68. [PubMed: 6345598]

Aston-Jones G, Waterhouse B. Locus coeruleus: From global projection system to adaptive regulation of behavior. Brain Research. 2016; 1645:75–78. [PubMed: 26969408]

Barrington FJ. The relation of the hind-brain to micturition. Brain. 1921; 44:23–53.

Barrington FJ. The effect of lesions of the hind- and mid-brain on micturition in the cat. Quarterly Journal of Experimental Physiology. 1925; 15:81–102.

Barrington FJ. Affections of micturition resulting from lesions of the nervous system. Proceedings of the Royal Society of Medicine. 1927; 20:722–727.

Blanco L, Yuste JE, Carrillo-de Sauvage MA, Gómez A, Fernández-Villalba E, Avilés-Olmos I, … Herrero MT. Critical evaluation of the anatomical location of the Barrington nucleus: Relevance for

deep brain stimulation surgery of pedunculopontine tegmental nucleus. Neuroscience. 2013; 247:351–363. [PubMed: 23732233]

Blok BF, de Weerd H, Holstege G. The pontine micturition center projects to sacral cord GABA immunoreactive neurons in the cat. Neuroscience Letters. 1997; 233:109–112. [PubMed: 9350844]

Blok BF, Holstege G. Ultrastructural evidence for a direct pathway from the pontine micturition center to the parasympathetic preganglionic motoneurons of the bladder of the cat. Neuroscience Letters. 1997; 222:195–198. [PubMed: 9148248]

Blok BF, van Maarseveen JT, Holstege G. Electrical stimulation of the sacral dorsal gray commissure evokes relaxation of the external urethral sphincter in the cat. Neuroscience Letters. 1998; 249:68–70. [PubMed: 9672391]

Boissard R, Fort P, Gervasoni D, Barbagli B, Luppi P-H. Localization of the GABAergic and non-GABAergic neurons projecting to the sublaterodorsal nucleus and potentially gating paradoxical sleep onset. The European journal of Neuroscience. 2003; 18:1627–1639. [PubMed: 14511341]

Boucher W, Kempuraj D, Michaelian M, Theoharides TC. Corticotropin-releasing hormone-receptor 2 is required for acute stress-induced bladder vascular permeability and release of vascular endothelial growth factor. BJU International. 2010; 106:1394–1399. [PubMed: 20201838]

Bruinstroop E, Cano G, VanderHorst VGJM, Cavalcante JC, Wirth J, Sena-Esteves M, Saper CB. Spinal projections of the A5, A6 (locus coeruleus), and A7 noradrenergic cell groups in rats. Journal of Comparative Neurology. 2012; 520:1985–2001. [PubMed: 22173709]

Carter ME, Yizhar O, Chikahisa S, Nguyen H, Adamantidis A, Nishino S, … de Lecea L. Tuning arousal with optogenetic modulation of locus coeruleus neurons. Nature Neuroscience. 2010; 13:1526–1533. [PubMed: 21037585]

Castaldi L. Studi sulla struttura e sullo sviluppo del mesencefalo. Richerche in Cavia cobaya. III. Archivio italiano di anatomia e di embriologia. Italian journal of anatomy and embryology. 1926; 23:481–609.

Chen P, Johnson JE, Zoghbi HY, Segil N. The role of Math1 in inner ear development: Uncoupling the establishment of the sensory primordium from hair cell fate determination. Development. 2002; 129:2495–2505. [PubMed: 11973280]

Chen Y, Lin Y-C, Kuo T-W, Knight ZA. Sensory detection of food rapidly modulates arcuate feeding circuits. Cell. 2015; 160:829–841. [PubMed: 25703096]

Curtis AL, Lechner SM, Pavcovich LA, Valentino RJ. Activation of the locus coeruleus noradrenergic system by intracoerulear microinfusion of corticotropin-releasing factor: Effects on discharge rate, cortical norepinephrine levels and cortical electroencephalographic activity. The Journal of Pharmacology and Experimental Therapeutics. 1997; 281:163–172. [PubMed: 9103494]

de Groat WC, Griffiths D, Yoshimura N. Neural control of the lower urinary tract. Comprehensive Physiology. 2015; 5:327–396. [PubMed: 25589273]

Dong, H-W. The Allen Institute for Brain Science. The Allen reference atlas. Hoboken: NJ: John Wiley & Sons; 2008.

Ennis M, Behbehani M, Shipley MT, Van Bockstaele EJ, Aston-Jones G. Projections from the periaqueductal gray to the rostromedial pericoerulear region and nucleus locus coeruleus: Anatomic and physiologic studies. The Journal of Comparative Neurology. 1991; 306:480–494. [PubMed: 1713927]

Fenno LE, Mattis J, Ramakrishnan C, Hyun M, Lee SY, He M, … Deisseroth K. Targeting cells with single vectors using multiple-feature Boolean logic. Nature Methods. 2014; 11:763–772. [PubMed: 24908100]

Fowler CJ, Griffiths D, de Groat WC. The neural control of micturition. Nature reviews Neuroscience. 2008; 9:453–466. [PubMed: 18490916]

Fowler CJ. Neurological disorders of micturition and their treatment. Brain. 1999; 122(Pt 7):1213–1231. [PubMed: 10388789]

Fujiyama T, Yamada M, Terao M, Terashima T, Hioki H, Inoue YU, … Hoshino M. Inhibitory and excitatory subtypes of cochlear nucleus neurons are defined by distinct bHLH transcription factors, Ptf1a and Atoh1. Development. 2009; 136:2049–2058. [PubMed: 19439493]

Garfield AS, Li C, Madara JC, Shah BP, Webber E, Steger JS, … Lowell BB. A neural basis for melanocortin-4 receptor-regulated appetite. Nature Neuroscience. 2015; 18:863–871. [PubMed: 25915476]

Geerling JC, Kim M, Mahoney CE, Abbott SBG, Agostinelli LJ, Garfield AS, … Scammell TE. Genetic identity of thermo-sensory relay neurons in the lateral parabrachial nucleus. American Journal of Physiology Regulatory, Integrative and Comparative Physiology. 2016; 310:R41–54.

Geerling JC, Loewy AD. Aldosterone-sensitive neurons in the nucleus of the solitary: Efferent projections. Journal of Comparative Neurology. 2006; 498:223–250. [PubMed: 16933386]

Geerling JC, Loewy AD. Sodium deprivation and salt intake activate separate neuronal subpopulations in the nucleus of the solitary tract and the parabrachial complex. Journal of Comparative Neurology. 2007; 504:379–403. [PubMed: 17663450]

Geerling JC, Shin J-W, Chimenti PC, Loewy AD. Para-ventricular hypothalamic nucleus: Axonal projections to the brainstem. Journal of Comparative Neurology. 2010; 518:1460–1499. [PubMed: 20187136]

Geerling JC, Stein MK, Miller RL, Shin J-W, Gray PA, Loewy AD. FoxP2 expression defines dorsolateral pontine neurons activated by sodium deprivation. Brain Research. 2011; 1375:19–27. [PubMed: 21108936]

Gompf HS, Mathai C, Fuller PM, Wood DA, Pedersen NP, Saper CB, Lu J. Locus ceruleus and anterior cingulate cortex sustain wakefulness in a novel environment. The Journal of Neuroscience: The Official Journal of the Society for Neuroscience. 2010; 30:14543–14551. [PubMed: 20980612]

Gray PA. Transcription factors and the genetic organization of brain stem respiratory neurons. Journal of Applied Physiology. 2008; 104:1513–1521. [PubMed: 18218908]

Gray PA. Transcription factors define the neuroanatomical organization of the medullary reticular formation. Frontiers in Neuroanatomy. 2013; 7:7. [PubMed: 23717265]

Grill WM, Bhadra N, Wang B. Bladder and urethral pressures evoked by microstimulation of the sacral spinal cord in cats. Brain Research. 1999; 836:19–30. [PubMed: 10415401]

Hallanger AE, Levey AI, Lee HJ, Rye DB, Wainer BH. The origins of cholinergic and other subcortical afferents to the thalamus in the rat. Journal of Comparative Neurology. 1987; 262:105–124. [PubMed: 2442206]

Hida T, Shimizu N. The interrelation between the laterodorsal tegmental area and lumbosacral segments of rats as studied by HRP method. Archivum Histologicum Japonicum = Nihon Soshikigaku Kiroku. 1982; 45:495–504. [PubMed: 7171292]

Hochbaum DR, Zhao Y, Farhi SL, Klapoetke N, Werley CA, Kapoor V, … Cohen AE. All-optical electrophysiology in mammalian neurons using engineered microbial rhodopsins. Nature Methods. 2014; 11:825–833. [PubMed: 24952910]

Holstege G, Griffiths D, de Wall H, Dalm E. Anatomical and physiological observations on supraspinal control of bladder and urethral sphincter muscles in the cat. Journal of Comparative Neurology. 1986; 250:449–461. [PubMed: 3760249]

Holstege G. How the emotional motor system controls the pelvic organs. Sexual Medicine Reviews. 2016; 4:303–328. [PubMed: 27872027]

Hoshino M, Nakamura S, Mori K, Kawauchi T, Terao M, Nishimura YV, … Nabeshima Y-I. Ptf1a, a bHLH transcriptional gene, defines GABAergic neuronal fates in cerebellum. Neuron. 2005; 47:201–213. [PubMed: 16039563]

Hou XH, Hyun M, Taranda J, Huang KW, Todd E, Feng D, … Sabatini BL. Central control circuit for context-dependent micturition. Cell. 2016; 167:73–86. e12. [PubMed: 27662084]

Imaki T, Nahan JL, Rivier C, Sawchenko PE, Vale W. Differential regulation of corticotropin-releasing factor mRNA in rat brain regions by glucocorticoids and stress. Journal of Neuroscience. 1991; 11:585–599. [PubMed: 2002354]

Jarvie BC, Palmiter RD. HSD2 neurons in the hindbrain drive sodium appetite. Nature Neuroscience. 2017; 20:167–169. [PubMed: 27918529]

Kabat H, Magoun HW, Ranson SW. Reaction of the bladder to stimulation of points in the forebrain and mid-brain. Journal of Comparative Neurology. 1936; 63:211–239.

Kiddoo DA, Valentino RJ, Zderic S, Ganesh A, Leiser SC, Hale L, Grigoriadis DE. Impact of state of arousal and stress neuropeptides on urodynamic function in freely moving rats. American Journal of Physiology. Regulatory, Integrative and Comparative Physiology. 2006; 290:R1697–706.

Klausner AP, Streng T, Na YG, Raju J, Batts TW, Tuttle JB, … Steers WD. The role of corticotropin releasing factor and its antagonist, astressin, on micturition in the rat. Autonomic Neuroscience: Basic & Clinical. 2005; 123:26–35. [PubMed: 16256445]

Komiyama A, Kubota A, Hidai H. Urinary retention associated with a unilateral lesion in the dorsolateral tegmentum of the rostral pons. Journal of Neurology, Neurosurgery, and Psychiatry. 1998; 65:953–954.

Koyama Y, Imada N, Kawauchi A, Kayama Y. Firing of putative cholinergic neurons and micturition center neurons in the rat laterodorsal tegmentum during distention and contraction of urinary bladder. Brain Research. 1999; 840:45–55. [PubMed: 10517951]

Koyama Y, Imada N, Kayama Y, Kawauchi A, Watanabe H. How does the distention of urinary bladder cause arousal? Psychiatry and Clinical Neurosciences. 1998; 52:142–145. [PubMed: 9628117]

Krashes MJ, Shah BP, Madara JC, Olson DP, Strochlic DE, Garfield AS, … Lowell BB. An excitatory paraventricular nucleus to AgRP neuron circuit that drives hunger. Nature. 2014; 507:238–242. [PubMed: 24487620]

Kruse MN, Mallory BS, Noto H, Roppolo JR, de Groat WC. Properties of the descending limb of the spinobulbospinal micturition reflex pathway in the cat. Brain Research. 1991; 556:6–12. [PubMed: 1933354]

Kuru M. Nervous control of micturition. Physiological Reviews. 1965; 45:425–494. [PubMed: 14340716]

Kuru M, Yamamoto H. Fiber connections of the pontine detrusor nucleus (Barrington). Journal of Comparative Neurology. 1964; 123:161–185. [PubMed: 14219662]

Lein ES, Hawrylycz MJ, Ao N, Ayres M, Bensinger A, Bernard A, … Jones AR. Genome-wide atlas of gene expression in the adult mouse brain. Nature. 2007; 445:168–176. [PubMed: 17151600]

Liu J, Willet SG, Bankaitis ED, Xu Y, Wright CVE, Gu G. Non-parallel recombination limits Cre-LoxP-based reporters as precise indicators of conditional genetic manipulation. Genesis. 2013; 51:436–442. [PubMed: 23441020]

Loewy AD, Saper CB, Baker RP. Descending projections from the pontine micturition center. Brain Research. 1979; 172:533–538. [PubMed: 476495]

Mallory B, Steers WD, De Groat WC. Electrophysiological study of micturition reflexes in rats. Am J Physiol. 1989; 257(2 Pt 2):R410–R421. [PubMed: 2764162]

Mallory BS, Roppolo JR, de Groat WC. Pharmacological modulation of the pontine micturition center. Brain Research. 1991; 546:310–320. [PubMed: 1676929]

Matsumoto G, Hisamitsu T, de Groat WC. Role of glutamate and NMDA receptors in the descending limb of the spinobulbospinal micturition reflex pathway of the rat. Neuroscience Letters. 1995; 183:58–61. [PubMed: 7746488]

McFadden K, Griffin TA, Levy V, Wolfe JH, Valentino RJ. Overexpression of corticotropin-releasing factor in Barrington's nucleus neurons by adeno-associated viral transduction: Effects on bladder function and behavior. The European journal of Neuroscience. 2012; 36:3356–3364. [PubMed: 22882375]

McKenna KE, Nadelhaft I. The organization of the pudendal nerve in the male and female rat. Journal of Comparative Neurology. 1986; 248:532–549. [PubMed: 3722467]

Million M, Wang L, Stenzel-Poore MP, Coste SC, Yuan PQ, Lamy C, … Taché Y. Enhanced pelvic responses to stressors in female CRF-overexpressing mice. American Journal of Physiology. Regulatory, Integrative and Comparative Physiology. 2007; 292:R1429–R1438.

Morin X, Cremer H, Hirsch MR, Kapur RP, Goridis C, Brunet JF. Defects in sensory and autonomic ganglia and absence of locus coeruleus in mice deficient for the homeobox gene Phox2a. Neuron. 1997; 18:411–423. [PubMed: 9115735]

Muglia L, Jacobson L, Dikkes P, Majzoub JA. Corticotropin-releasing hormone deficiency reveals major fetal but not adult glucocorticoid need. Nature. 1995; 373:427–432. [PubMed: 7830793]

Nadelhaft I, Vera PL. Neurons in the rat brain and spinal cord labeled after pseudorabies virus injected into the external urethral sphincter. Journal of Comparative Neurology. 1996; 375:502–517. [PubMed: 8915845]

Nishizawa O, Sugaya K, Noto H, Harada T, Tsuchida S. Pontine micturition center in the dog. The Journal of Urology. 1988; 140:872–874. [PubMed: 3418825]

Noto H, Roppolo JR, Steers WD, de Groat WC. Excitatory and inhibitory influences on bladder activity elicited by electrical stimulation in the pontine micturition center in the rat. Brain Research. 1989; 492:99–115. [PubMed: 2752312]

Noto H, Roppolo JR, Steers WD, de Groat WC. Electrophysiological analysis of the ascending and descending components of the micturition reflex pathway in the rat. Brain Research. 1991; 549:95–105. [PubMed: 1893257]

Page ME, Akaoka H, Aston-Jones G, Valentino RJ. Bladder distention activates noradrenergic locus coeruleus neurons by an excitatory amino acid mechanism. Neuroscience. 1992; 51:555–563. [PubMed: 1336819]

Pang YW, Li J-L, Nakamura K, Wu S, Kaneko T, Mizuno N. Expression of vesicular glutamate transporter 1 immunoreactivity in peripheral and central endings of trigeminal mesencephalic nucleus neurons in the rat. Journal of Comparative Neurology. 2006; 498:129–141. [PubMed: 16856164]

Pattyn A, Goridis C, Brunet JF. Specification of the central noradrenergic phenotype by the homeobox gene Phox2b. Molecular and Cellular Neurosciences. 2000; 15:235–243. [PubMed: 10736201]

Pavcovich LA, Valentino RJ. Central regulation of micturition in the rat the corticotropin-releasing hormone from Barrington's nucleus. Neuroscience Letters. 1995; 196:185–188. [PubMed: 7501279]

Paxinos, G., Franklin, KBJ. The mouse brain in stereotaxic coordinates. 4. Cambridge: MA: Academic Press; 2008. p. 68-86.

Paxinos, G., Watson, C. The rat brain in stereotaxic coordinates. Cambridge: MA: Academic Press; 2006.

Peoples JF, Wessendorf MW, Pierce T, Van Bockstaele EJ. Ultrastructure of endomorphin-1 immunoreactivity in the rat dorsal pontine tegmentum: Evidence for preferential targeting of peptidergic neurons in Barrington's nucleus rather than catecholaminergic neurons in the peri-locus coeruleus. Journal of Comparative Neurology. 2002; 448:268–279. [PubMed: 12115708]

Petreanu L, Huber D, Sobczyk A, Svoboda K. Channelrhodopsin-2-assisted circuit mapping of long-range callosal projections. Nature Neuroscience. 2007; 10:663–668. [PubMed: 17435752]

Proudfit WL, Forteza ME. Micturition syncope. The New England Journal of Medicine. 1959; 260:328–331. [PubMed: 13632886]

Rizvi TA, Ennis M, Aston-Jones G, Jiang M, Liu WL, Behbehani MM, Shipley MT. Preoptic projections to Barrington's nucleus and the pericoerulear region: Architecture and terminal organization. Journal of Comparative Neurology. 1994; 347:1–24. [PubMed: 7528227]

Rose MF, Ahmad KA, Thaller C, Zoghbi HY. Excitatory neurons of the proprioceptive, interoceptive, and arousal hindbrain networks share a developmental requirement for Math1. Proceedings of the National Academy of Sciences of the United States of America. 2009; 106:22462–22467. [PubMed: 20080794]

Rouzade-Dominguez M-L, Pernar L, Beck S, Valentino RJ. Convergent responses of Barrington's nucleus neurons to pelvic visceral stimuli in the rat: A juxtacellular labelling study. The European journal of Neuroscience. 2003; 18:3325–3334. [PubMed: 14686905]

Sakakibara R. Lower urinary tract dysfunction in patients with brain lesions. Handbook of Clinical Neurology. 2015; 130:269–287. [PubMed: 26003249]

Saper CB, Scammell TE, Lu J. Hypothalamic regulation of sleep and circadian rhythms. Nature. 2005; 437:1257–1263. [PubMed: 16251950]

Satoh K, Shimizu N, Tohyama M, Maeda T. Localization of the micturition reflex center at dorsolateral pontine tegmentum of the rat. Neuroscience Letters. 1978; 8:27–33. [PubMed: 19605144]

Satoh K, Tohyama M, Sakumoto T, Yamamoto K, Shimizu N. Descending projection of the nucleus tegmentalis laterodorsalis to the spinal cord; studied by the horseradish peroxidase method

following 6-hydroxy-DOPA administration. Neuroscience Letters. 1978; 8:9–15. [PubMed: 19605141]

Shin J-W, Geerling JC, Stein MK, Miller RL, Loewy AD. FoxP2 brainstem neurons project to sodium appetite regulatory sites. Journal of Chemical Neuroanatomy. 2011; 42:1–23. [PubMed: 21605659]

Sie JA, Blok BF, de Weerd H, Holstege G. Ultrastructural evidence for direct projections from the pontine micturition center to glycine-immunoreactive neurons in the sacral dorsal gray commissure in the cat. Journal of Comparative Neurology. 2001; 429:631–637. [PubMed: 11135240]

Srinivas S, Watanabe T, Lin CS, William CM, Tanabe Y, Jessell TM, Costantini F. Cre reporter strains produced by targeted insertion of EYFP and ECFP into the ROSA26 locus. BMC Developmental Biology. 2001; 1:4. [PubMed: 11299042]

Standaert DG, Needleman P, Saper CB. Organization of atriopeptin-like immunoreactive neurons in the central nervous system of the rat. Journal of Comparative Neurology. 1986; 253:315–341. [PubMed: 2947936]

Stornetta RL, Sevigny CP, Guyenet PG. Vesicular glutamate transporter DNPI/VGLUT2 mRNA is present in C1 and several other groups of brainstem catecholaminergic neurons. Journal of Comparative Neurology. 2002; 444:191–206. [PubMed: 11840474]

Sugaya K, Matsuyama K, Takakusaki K, Mori S. Electrical and chemical stimulations of the pontine micturition center. Neuroscience Letters. 1987; 80:197–201. [PubMed: 3683977]

Swanson, LW. Brain maps. Cambridge: MA: Elsevier Academic Press; 2004.

Swanson LW, Sawchenko PE, Rivier J, Vale WW. Organization of ovine corticotropin-releasing factor immunoreactive cells and fibers in the rat brain: An immunohistochemical study. Neuroendocrinology. 1983; 36:165–186. [PubMed: 6601247]

Tallini YN, Shui B, Greene KS, Deng K-Y, Doran R, Fisher PJ, … Kotlikoff MI. BAC transgenic mice express enhanced green fluorescent protein in central and peripheral cholinergic neurons. Physiological Genomics. 2006; 27:391–397. [PubMed: 16940431]

Tamamaki N, Yanagawa Y, Tomioka R, Miyazaki J-I, Obata K, Kaneko T. Green fluorescent protein expression and colocalization with calretinin, parvalbumin, and somatostatin in the GAD67-GFP knock-in mouse. Journal of Comparative Neurology. 2003; 467:60–79. [PubMed: 14574680]

Tanaka Y, Koyama Y, Kayama Y, Kawauchi A, Ukimura O, Miki T. Firing of micturition center neurons in the rat mesopontine tegmentum during urinary bladder contraction. Brain Research. 2003; 965:146–154. [PubMed: 12591131]

Tang PC. Levels of brain stem and diencephalon controlling micturition reflex. Journal of Neurophysiology. 1955; 18:583–595. [PubMed: 13272043]

Tohyama M, Satoh K, Sakumoto T, Kimoto Y, Takahashi Y, Yamamoto K, Itakura T. Organization and projections of the neurons in the dorsal tegmental area of the rat. Journal fur Hirnforschung. 1978; 19:165–176. [PubMed: 690413]

Ueki K. Disturbances in some patients with brain tumor. Neurologica Medico Chirurgica. 1960; 2:25–33.

Valentino RJ, Page ME, Luppi PH, Zhu Y, Van Bockstaele E, Aston-Jones G. Evidence for widespread afferents to Barrington's nucleus, a brainstem region rich in corticotropin-releasing hormone neurons. Neuroscience. 1994; 62:125–143. [PubMed: 7816195]

Valentino RJ, Pavcovich LA, Hirata H. Evidence for corticotropin-releasing hormone projections from Barrington's nucleus to the periaqueductal gray and dorsal motor nucleus of the vagus in the rat. Journal of Comparative Neurology. 1995; 363:402–422. [PubMed: 8847408]

VanderHorst VGJM, Gustafsson J-A, Ulfhake B. Estrogen receptor-alpha and -beta immunoreactive neurons in the brainstem and spinal cord of male and female mice: Relationships to monoaminergic, cholinergic, and spinal projection systems. Journal of Comparative Neurology. 2005; 488:152–179. [PubMed: 15924341]

VanderHorst VGJM, Ulfhake B. The organization of the brainstem and spinal cord of the mouse: Relationships between monoaminergic, cholinergic, and spinal projection systems. Journal of Chemical Neuroanatomy. 2006; 31:2–36. [PubMed: 16183250]

Vincent SR, Satoh K. Corticotropin-releasing factor (CRF) immunoreactivity in the dorsolateral pontine tegmentum: Further studies on the micturition reflex system. Brain Research. 1984; 308:387–391. [PubMed: 6383518]

Vong L, Ye C, Yang Z, Choi B, Chua S, Lowell BB. Leptin action on GABAergic neurons prevents obesity and reduces inhibitory tone to POMC neurons. Neuron. 2011; 71:142–154. [PubMed: 21745644]

Wang L, Goebel-Stengel M, Stengel A, Wu SV, Ohning G, Taché Y. Comparison of CRF-immunoreactive neurons distribution in mouse and rat brains and selective induction of Fos in rat hypothalamic CRF neurons by abdominal surgery. Brain Research. 2011; 1415:34–46. [PubMed: 21872218]

Wickersham IR, Lyon DC, Barnard RJO, Mori T, Finke S, Conzelmann K-K, … Callaway EM. Monosynaptic restriction of transsynaptic tracing from single, genetically targeted neurons. Neuron. 2007; 53:639–647. [PubMed: 17329205]

Yamada M, Seto Y, Taya S, Owa T, Inoue YU, Inoue T, … Hoshino M. Specification of spatial identities of cerebellar neuron progenitors by ptf1a and atoh1 for proper production of GABAergic and glutamatergic neurons. The Journal of Neuroscience: The Official Journal of the Society for Neuroscience. 2014; 34:4786–4800. [PubMed: 24695699]

Yamao Y, Koyama Y, Akihiro K, Yukihiko K, Tsuneharu M. Discrete regions in the laterodorsal tegmental area of the rat regulating the urinary bladder and external urethral sphincter. Brain Research. 2001; 912:162–170. [PubMed: 11532432]

Yoshimura N, Sasa M, Yoshida O, Takaori S. Mediation of micturition reflex by central norepinephrine from the locus coeruleus in the cat. The Journal of Urology. 1990; 143:840–843. [PubMed: 2107337]

Yoshiyama M, Roppolo JR, de Groat WC. Interactions between NMDA and AMPA/kainate receptors in the control of micturition in the rat. European Journal of pharmacology. 1995; 287:73–78. [PubMed: 8666029]

Zanoli P, Ferrari W. Effect of colchicine on micturition reflex in rats. Neurotoxicology and Teratology. 1988; 10:579–584. [PubMed: 3244348]

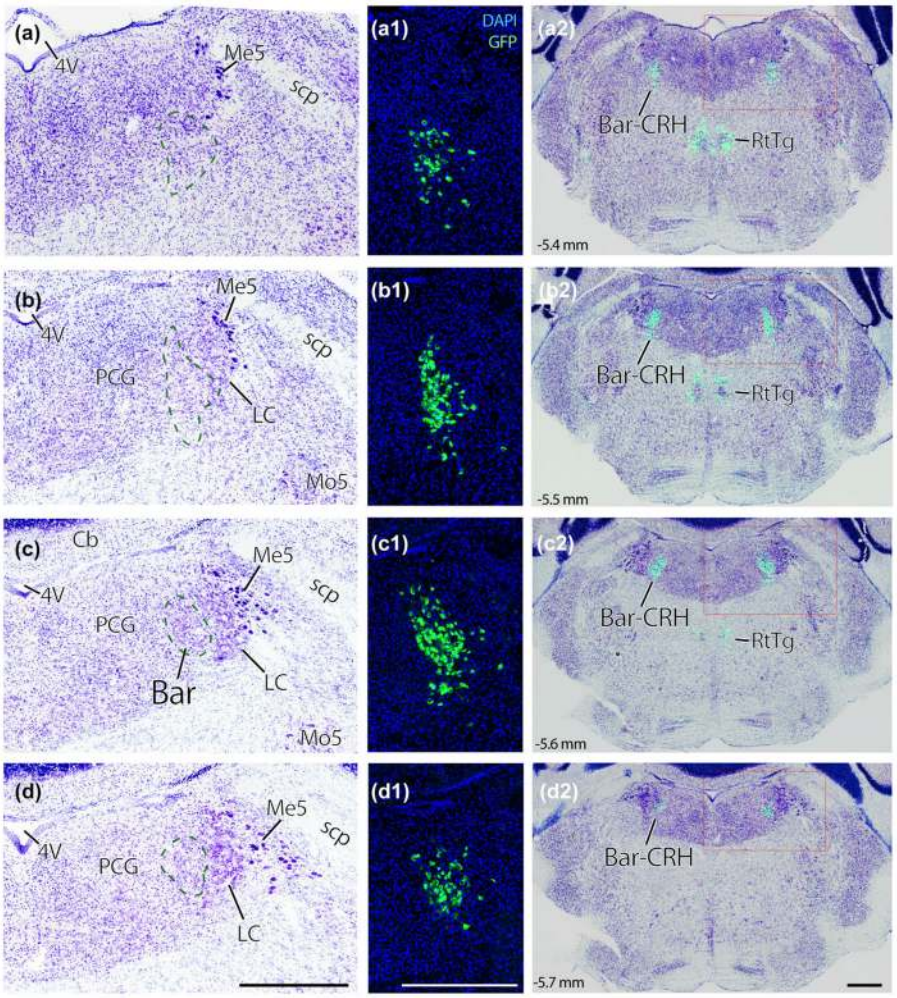

FIGURE 1.

Nissl cytoarchitecture in the mouse brainstem region that contains Barrington's nucleus (Bar). Panels (a–d): successive rostral-to-caudal sections through the pons of a *Crh* reporter mouse. Every third section (35 μm-thick) is shown across a total span of ~0.5 mm. Bar neurons, using Nissl cytoarchitecture alone, are evident as an ovoid cluster of medium-large neurons located medial to the ventral locus coeruleus (dashed line in panel c). Rostral and caudal to this core, we cannot distinguish Bar neurons from surrounding populations in a Nissl preparation. Panels (a1–d1) show a GFP reporter for *Crh* in the same tissue sections as (a–d), at the same magnification, in fluorescence images taken prior to Nissl counterstaining. The location of Bar^{CRH} neurons in each section is indicated by a green dashed line in panels (a–d). Panels (a2–d2) show the distribution of Bar^{CRH} neurons throughout each section by blending images of GFP and thionin counterstaining from the same sections. Scale bars are all 500 μm (d–d2), and apply to the column above. Approximate level in mm caudal to bregma is shown in the lower left corner of panels (a2–d2) and applies to all panels in each row. 4V = fourth ventricle; Bar-CRH = corticotropin releasing hormone neurons in Barrington's nucleus; LC = locus coeruleus; Me5 = mesencephalic nucleus and tract of the

trigeminal nerve; Mo5 = motor nucleus of the trigeminal nerve. PCG = pontine central gray matter; RtTg = reticular tegmental nucleus; scp, superior cerebellar peduncle

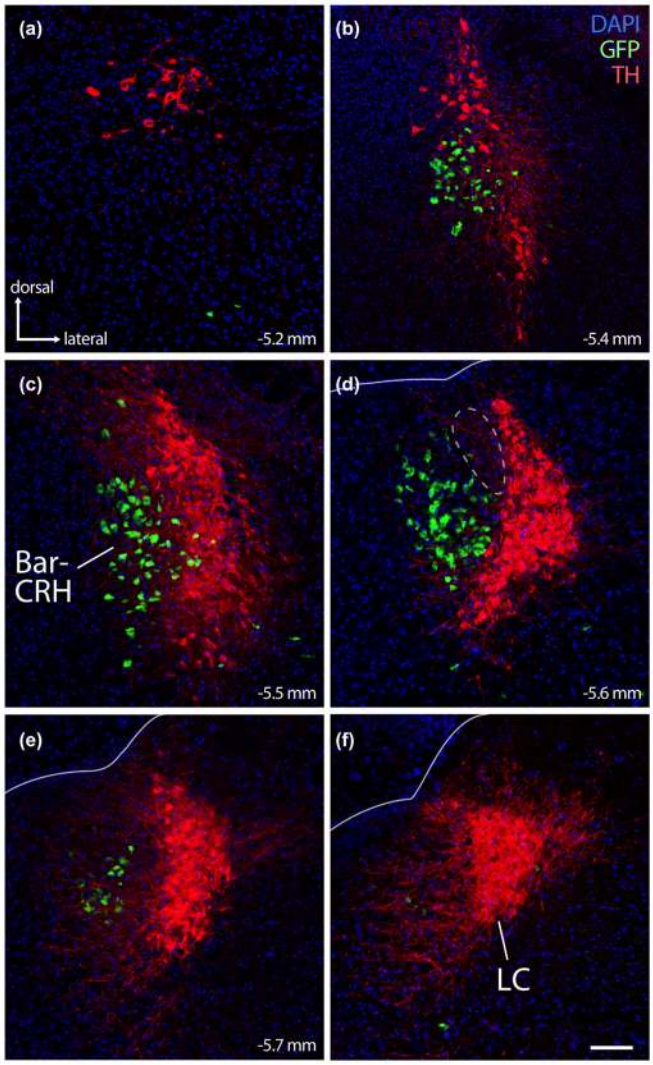

FIGURE 2.

The crescent-shaped locus coeruleus (LC) cradles the lateral surface of mouse Bar^{CRH} neurons. Panels (a–f) show the close relationship between LC (immunofluorescence labeling for tyrosine hydroxylase; TH, red) and Bar^{CRH} (GFP reporter for *Crh*, green). Bar^{CRH} neurons are found at middle-to-rostral levels of the LC (panels B–E, corresponding to the same approximate bregma levels as Figure 1, panels a–d). No neurons are double-labeled. Rostral to the LC, there are no more Bar^{CRH} neurons, though sparse, large neurons immunoreactive for TH extend rostrally into the periaqueductal gray. At caudal levels (panels e, f), there are few or no Bar^{CRH} neurons. At these caudal levels, LC dendrites project medially into a zone immediately behind the core of Bar. At central levels containing the core of Bar (panel d), its dorsolateral surface diverges from the dorsal LC; the resulting gap between Bar^{CRH} and the dorsal LC (dashed outline in panel d) is filled by a wedge of FoxP2/glutamatergic neurons, which are shown in Figure 6. Lines in panels (d–f) mark the ependymal surface of the fourth ventricle. Scale bar is 100 μm and applies to all panels

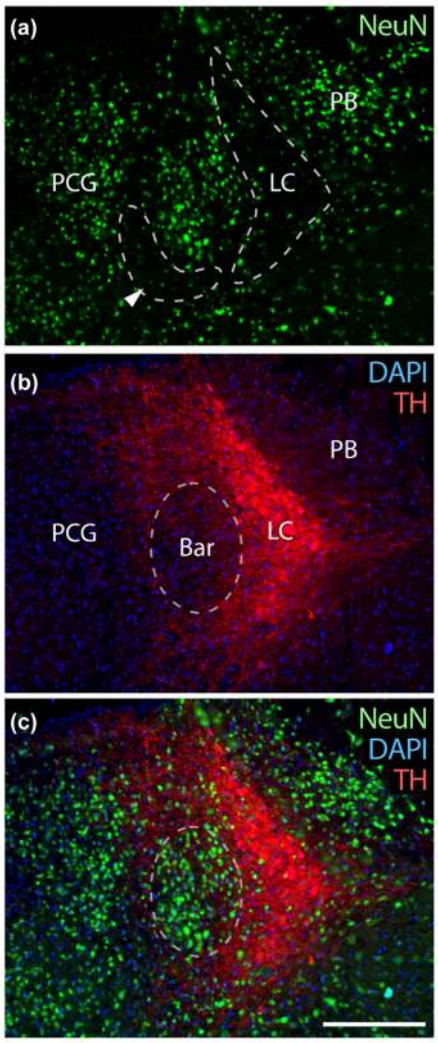

FIGURE 3.

Bar neurons have prominent NeuN nuclear immunoreactivity. (a) NeuN immunofluorescence (green) is prominent in many neurons in the pontine tegmentum, including the PB and pontine central gray (PCG) medial to Bar. However, NeuN is not ubiquitous, and most LC neurons lack it. It is also largely absent in the region bordering Bar on its ventromedial surface (arrowhead). (b) TH-immunofluorescence (red) is shown for reference, showing LC neurons and their dendrites projecting medially above and below Bar. (c) Shows NeuN and TH in combination with DAPI nuclear staining for all cells. Scale bar is 200 μm

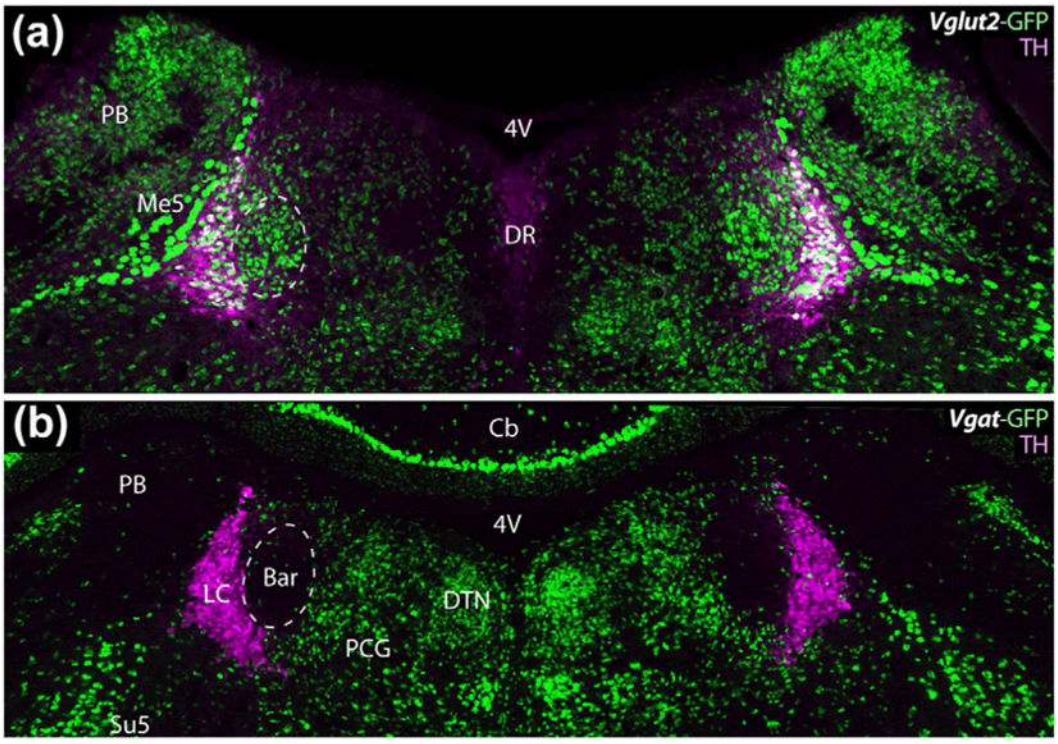

FIGURE 4.

Bar contains predominantly glutamatergic neurons, as shown by the presence of a GFP reporter for the type 2 vesicular glutamate transporter (*Vglut2*), and absence of a reporter for the vesicular GABA/glycine transporter (*Vgat*). Panels (a) and (b) compare the distributions of *Vglut2* (glutamatergic) and *Vgat* (GABAergic/glycinergic) neurons, respectively, in the pontine tegmentum at levels containing the core of Bar. TH immunofluorescence (magenta) is labeled as a landmark. The core of Bar contains a prominent cluster of glutamatergic neurons, and is virtually devoid of GABAergic neurons. Conversely, a region of the pontine central gray (PCG) just medial and ventral to Bar contains many *Vgat*/GABAergic neurons and relatively few *Vglut2*/glutamatergic neurons. Scale bar in (b) is 200 μm and applies to both panels. Additional abbreviations: Cb = cerebellum; DR = dorsal raphe nucleus; DTN = dorsal tegmental nucleus; Me5 = mesencephalic trigeminal nucleus; Su5 = supratrigeminal nucleus

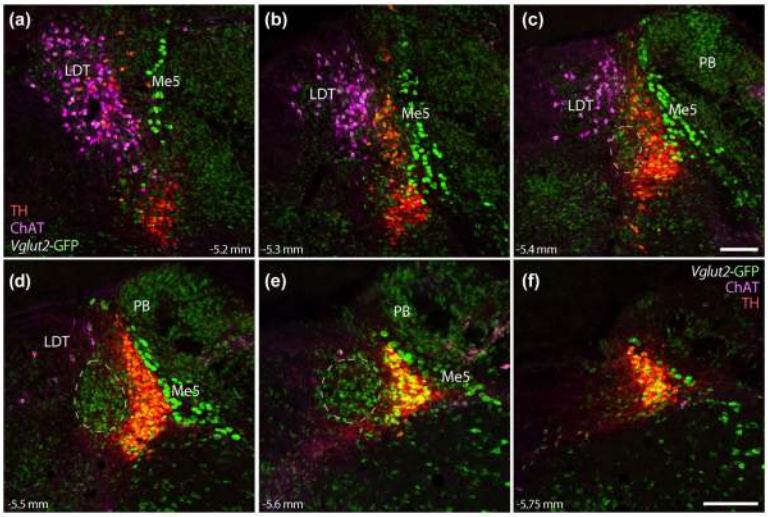

FIGURE 5.

Glutamatergic neurons in Bar are surrounded by mutually exclusive populations of cholinergic and catecholaminergic neurons, as well as other glutamatergic populations. Panels (a–f) show, in successive rostral to caudal levels, the relative positions of neurons in each population. Laterodorsal tegmental nucleus (LDT) neurons, labeled by immunofluorescence for choline acetyltransferase (ChAT, magenta), are located rostral and medial-dorsal to Bar. *Vglut2* GFP reporter is found in many LC catecholaminergic (red +green = yellow) and LDT cholinergic neurons (magenta +green = white), as well the large Me5 neurons dorsolateral to the LC, and most neurons in the PB. The dashes in panels (c–e) outline the approximate location of Bar, estimated from the distribution of Bar^{CRH} neurons shown above. Scale bars are all 200 μm (panel c applies to a–c; panel f applies to d–f). Approximate levels in mm caudal to bregma are given at the bottom left or right of each panel

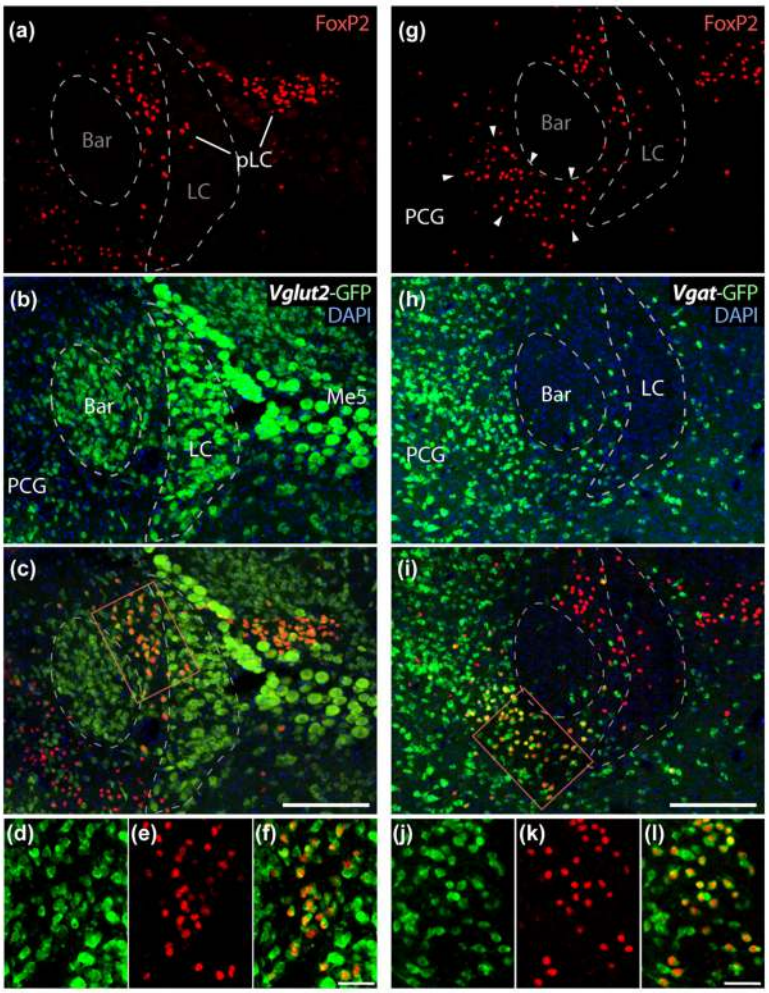

FIGURE 6.

Bar is surrounded by two populations of neurons that express FoxP2. (a–c) At its dorsolateral surface, Bar borders a cluster of small neurons with FoxP2-immunoreactive nuclei (red) and GFP reporter for *Vglut2* (but not for *Vgat*, see panel i). This population of FoxP2/*Vglut2* neurons is referred to as the pre-LC (pLC), and forms a wedge between Bar and dorsal LC, corresponding to the dashed outline in Figure 2d; pLC neurons also distribute laterally through the LC and Me5 and into the medial PB. Panels (d–f) the double-labeling for FoxP2 and GFP (reporter for *Vglut2*) in a subset of these neurons. (g–i) Across from the pLC, Bar borders a separate cluster of FoxP2-expressing neurons. These neurons fill a region lacking NeuN (highlighted in Figure 3) and are a subset of the larger population of GABAer-gic neurons in the pontine central gray (PCG). They express GFP reporter for *Vgat* (but not for *Vglut2*, see panel c). Panels (j–l) show double-labeling for FoxP2 and GFP (reporter for *Vgat*) in a subset of these neurons. Scale bars are 200 μm in panels (c and i) and 50 μm in panels (f and l)

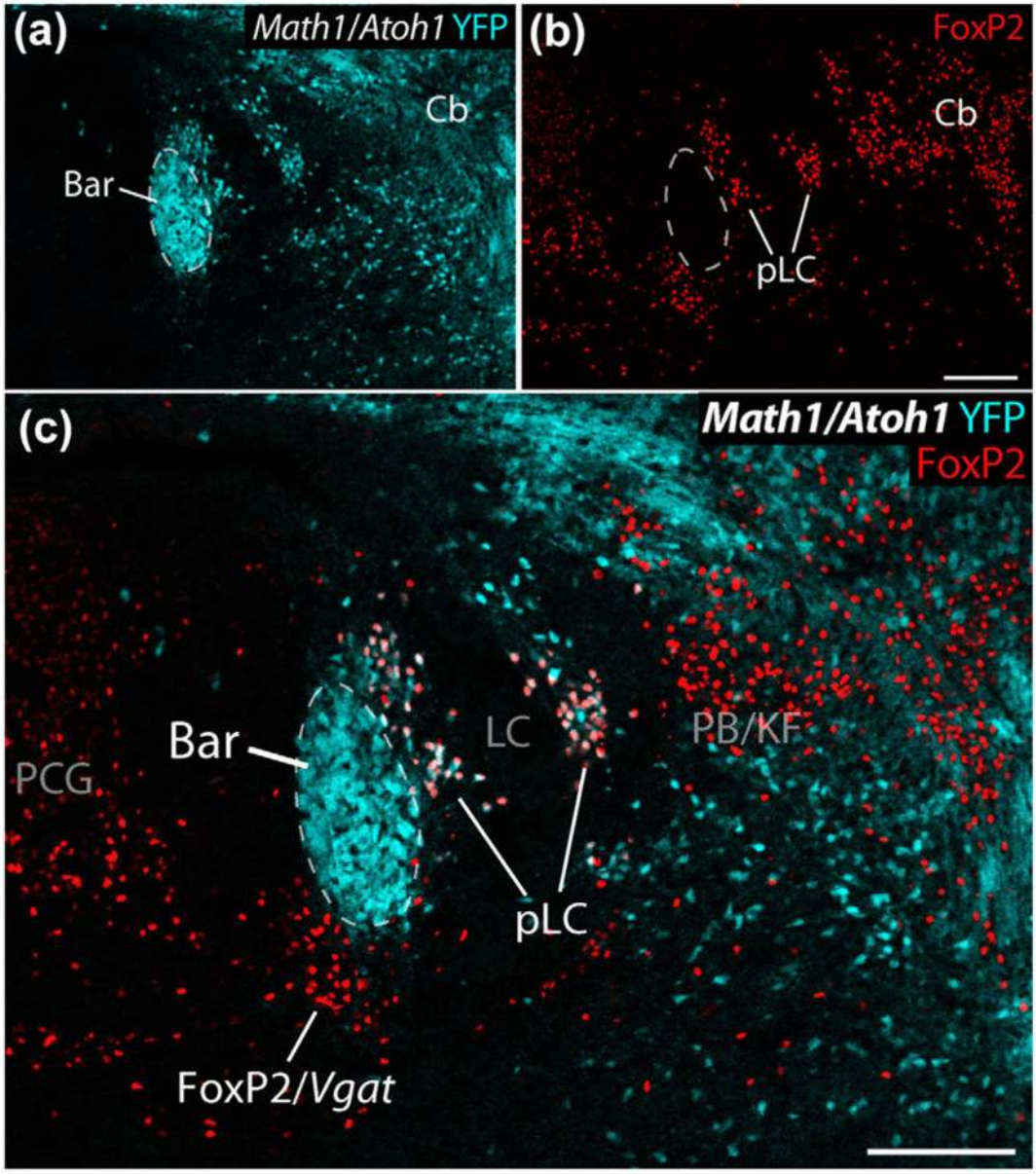

FIGURE 7.

In this Cre-reporter mouse (*Atoh1-Cre; R26-lsl-YFP*), YFP expression (ice-blue) reveals cells derived from embryonic *Math1*/*Atoh1*-expressing precursors in the rhombic lip neurothelium in a P0 mouse. Among the *Math1*/*Atoh1*-derived neurons in the pontine tegmentum are a dense cluster with the expected location, size, and shape of Bar. These images also contain FoxP2 immunolabeling (red) in cells surrounding Bar. LC neurons, which are derived from separate precursors, do not express YFP. Cerebellar cells (granule cell precursors) and other neurons express YFP, including FoxP2 (pLC) neurons bordering the dorsolateral surface of Bar and winding through the LC. In contrast, FoxP2 neurons in the PCG, including those bordering the ventromedial surface of Bar (FoxP2/ *Vgat*), do not express YFP. Other populations highlighted in this image include a group of non-*Math1*/

Atoh1-derived, FoxP2+ neurons in the caudal PB/Kolliker-Fuse nucleus (PB/KF), which are GABAergic and are separate from the larger population of *Math1*-derived (glutamatergic) FoxP2 expressing neurons through much of the PB found at levels rostral to this. Scale bars in panels (b) and (c) are 200 μm

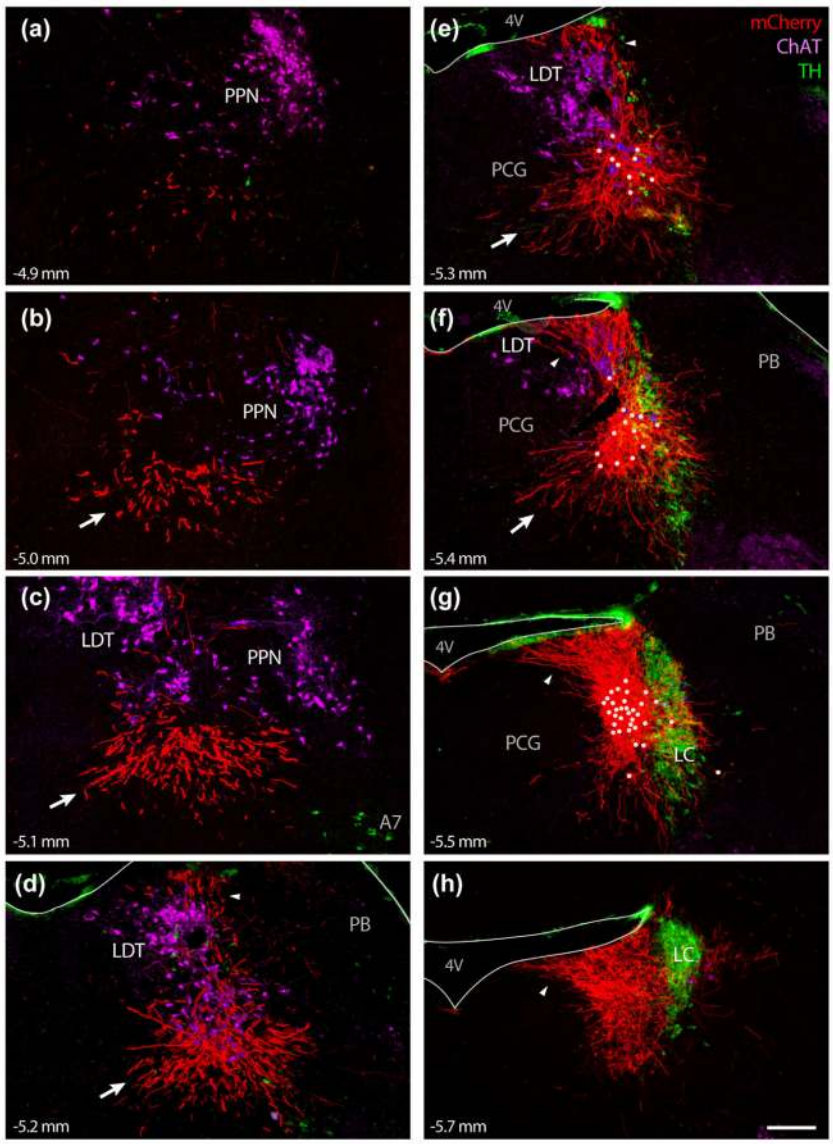

FIGURE 8.

The dendritic arbors of Bar^{CRH} neurons are extensive, and may receive synaptic inputs up to 500 μm outside the cytoarchitectural borders of Bar. Panels (a–h) show successive rostral-to-caudal levels of the caudal midbrain (a–c) and pontine tegmentum (d–h) of mice expressing a membrane-targeted fluorescent protein in Bar^{CRH} neurons (Cre-dependent hM3Dq-mCherry in a *Crh-IRES-Cre* mouse). Cell bodies expressing mCherry (white dots) were concentrated in or near Bar and were few in number, yet extend thick, brightly labeled dendritic processes primarily in three directions: (1) Rostral- medial, extending as far as to 500 μm along the ventral aspect of cholinergic neurons in the LDT and pedunculopontine tegmental nucleus (PPN); this dendritic bundle is indicated by white arrows in panels (b–f). (2) Dorsal, extending up to and fanning out along the fourth ventricle (4V) ependyma (highlighted by arrowheads in panels d–h). And (3) caudal, producing an extensive dendritic arbor immediately behind Bar^{CRH} cell bodies and overlapping some dendrites that extend medially from neurons in the caudal LC. Smaller numbers of Bar^{CRH} dendrites project

ventrally or laterally around and through the LC (f–g). The scale bar (panel h) is 200 μm and applies to all panels. TH was labeled in this case with a mouse monoclonal antibody that also cross-reacts with an antigen in the pia and ependyma, producing green immunofluorescence lining the 4V (d–h) and brainstem surface dorsolateral to the PB (d–g). Approximate level in mm caudal to bregma is given in the lower left corner of each panel

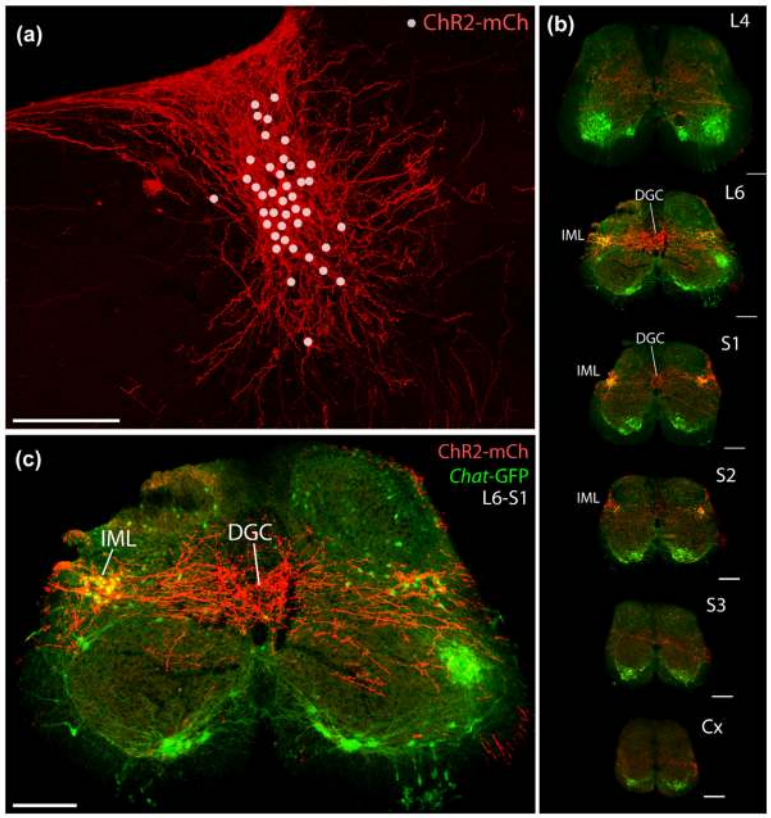

FIGURE 9.

ChR2-mCherry expressed selectively in Bar^{CRH} neurons after injecting AAV into a *Crh-IRES-Cre; Chat-GFP* mouse, which also expresses GFP in cholinergic neurons. (a) In addition to cell bodies (marked with dots) and dendrites, ChR2-mCherry robustly labels axons projecting to the spinal cord (b, c). Upon reaching low lumbar and upper sacral levels, Bar^{CRH} axons ramify extensively in a horizontal stripe that envelops two major targets: (1) cholinergic neurons (green) in the intermediolateral nucleus (IML) and (2) a large region of the central gray matter known as the dorsal gray commissure (DGC). All scale bars are 200 μm. Spinal cord sections in (b) were scaled proportionally and assigned approximate lumbar (L), sacral (S), and coccygeal (Cx) levels

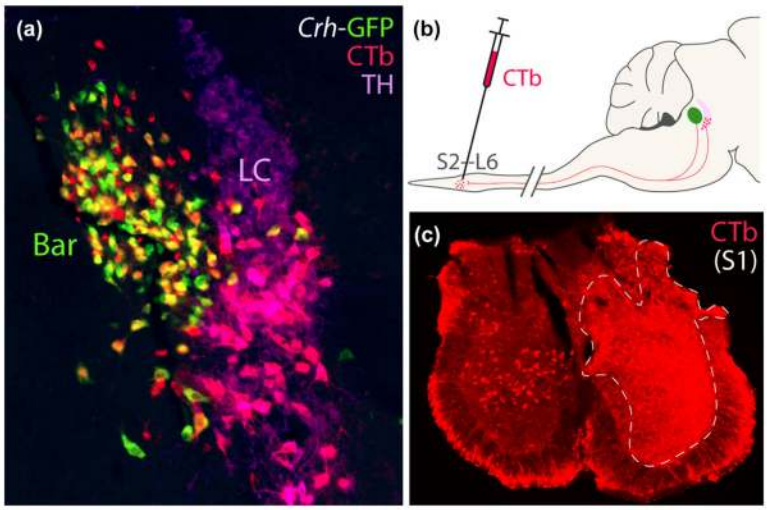

FIGURE 10.

Injecting CTb into the lumbosacral spinal cord retrogradely labels neurons in Bar and LC. (a) In this CRH reporter mouse (*Crh-IRES-Cre; L10-GFP*), a slight majority of retrogradely labeled neurons in Bar express GFP. These CTb-labeled, Bar^{CRH} neurons appear yellow-orange due to labeling for both CTb (red) and GFP (green). Outside Bar, CTb-labeled neurons were located in the ventral LC and subcoeruleus, and all of them express TH. CTb-labeled LC neurons appear pink due to labeling for both CTb (red) and TH (magenta). The diagram in panel (b) shows the CTb injection located in the lumbosacral spinal cord. Panel (c) shows a level of the sacral spinal cord in this mouse at the center of the injection site resulting in the ipsilateral, retrograde labeling shown in (a); the contralateral sacral gray matter contains several CTb retrogradely labeled neurons. Scale bars are 200 μm

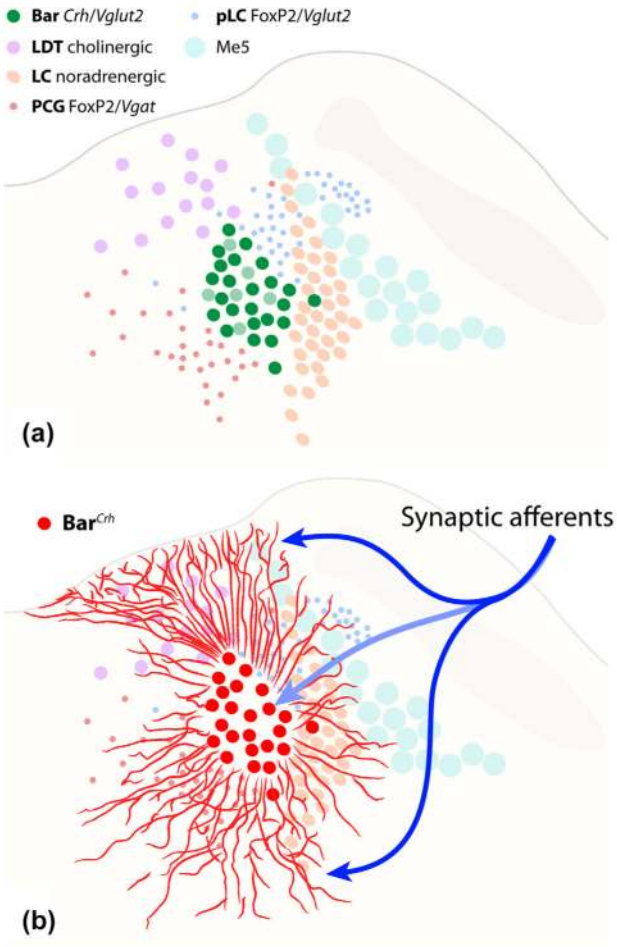

FIGURE 11.

Summary drawings of the mouse pontine tegmentum show (a) the relative distributions of neurons in Bar and five surrounding populations and (b) the unexpectedly large territory covered by dendritic processes emerging from Bar^{CRH} neurons (as in Figure 8). These long dendrites may receive a broader range of synaptic (input) connections than those identified in previous tracing studies targeting the somatic core. The neuron populations abbreviated in the legend (a) are detailed in the text and figures above

TABLE 1

Antisera used in this study

Antigen	Description of immunogen	Source, host species, Cat. #, RRID	Concentration
CTb	Purified choleragenoid, the B subunit of cholera toxin	List Biological, goat polyclonal, cat. #703, lot #115037, RRID: AB_10013220	1:5,000 1:2,000
ChAT	Human placental choline acetyltransferase	Millipore, goat polyclonal, #AB144P, RRID: AB_2079751	1:500
dsRed	DsRed-Express, a variant of *Discosoma sp.* red fluorescent protein	Clontech, rabbit polyclonal, cat. # 632496, RRID: AB_10015246	1:2,000
GFP (adult) GFP (P0)	GFP isolated directly from the jellyfish *Aequorea victoria* Recombinant GFP protein	Invitrogen, chicken polyclonal, cat. #A10262, RRID: AB_ 2534023 Aves labs, chicken polyclonal, cat. #GFP-1020, RRID: AB_10000240	1:2,000 1:1,000
mCherry	Fully length mCherry fluorescent protein	Life Sciences, rat monoclonal, cat. #M11217, RRID: AB_2536611	1:1,000
NeuN	Purified cell nuclei from mouse brain	Millipore, mouse monoclonal (clone A60), cat. #MAB377, RRID: AB_2298772	1:500
TH	Purified, SDS-denatured rat pheochromocytoma tyrosine hydroxylase	Millipore, mouse monoclonal, cat. #657010, RRID: AB_212601 Millipore, sheep polyclonal, cat. #AB1542, RRID: AB_11213126 Millipore, rabbit polyclonal, cat. #657012, RRID: AB_566341	1:1,000 1:2,000 1:2,500
FoxP2 FoxP2 (P0)	Recombinant peptide sequence corresponding to Ala640-Glu715 of human FoxP2 Synthetic peptide: REIEEEPLSEDLE, corresponding to C terminal amino acids 703–715 of Human FOXP2.	R&D Systems, sheep polyclonal, cat. #AF5647, RRID: AB_2107133 Abcam, goat polyclonal, cat #ab1307, RRID: AB_1268914	1:4,000 1:2,000